one-electron reduction is essentially metal-based and results in a more traditional $19e^-d^9$ complex lacking a high degree of delocalization onto the cyclooctatetraene ring, just as is obtained, for example, with simple metal-diolefin compounds.[65]

(65) Leading references to d^9 π-hydrocarbon complexes may be found in refs 25, 54, 58, and 59. Note that the possibility of electron-transfer-induced isomerization of a metal-cyclooct*adiene* bond is raised in refs 11b, 25, and in Baghdadi, J.; Bailey, N. A.; Dowding, A. S.; White, C. *J. Chem. Soc., Chem. Commun.* **1992**, 170.

Acknowledgment. W.E.G. is grateful for the support of the National Science Foundation under CHE86-03728 and CHE91-16332. We thank Thomas C. Richards for obtaining the new ESR spectrum of $CpCo(1,3\text{-}C_8H_8)^-$.

Note Added in Proof. Koelle et al., in ref 48c, have recently interpreted the ESR spectra of $CpNi(C_8H_{12})$ in a $CpCo(C_8H_{12})$ matrix in terms of a metal d_{xz} ground state, with the d_{yz} level lying just below.

Synthesis, Structure, and Spectroscopic Properties of Chiral Rhenium Aromatic Aldehyde Complexes $[(\eta^5\text{-}C_5H_5)Re(NO)(PPh_3)(O{=}CHAr)]^+X^-$: Equilibria between π and σ Aldehyde Binding Modes

N. Quirós Méndez, Jeffery W. Seyler, A. M. Arif, and J. A. Gladysz*

Contribution from the Department of Chemistry, University of Utah, Salt Lake City, Utah 84112.
Received September 24, 1992

Abstract: Reactions of $[(\eta^5\text{-}C_5H_5)Re(NO)(PPh_3)(ClCH_2Cl)]^+BF_4^-$ and ArCHO (Ar = **a**, C_6F_5; **b**, 4-$C_6H_4CF_3$; **c**, 3-$C_6H_4CF_3$; **d**, 3-$C_6H_4OCH_3$; **e**, 2-$C_6H_4OCH_3$; **f**, 4-C_6H_4Cl; **g**, 4-C_6H_4F; **h**, 1-naphthyl; **i**, C_6H_5; **j**, 3,4,5-$C_6H_2(OCH_3)_3$; **k**, 4-$C_6H_4C_6H_5$; **l**, 4-$C_6H_4CH_3$; **m**, 2,4-$C_6H_3(OCH_3)_2$; n, 3,4-$C_6H_3(OCH_3)_2$; o, 4-$C_6H_4OCH_3$) give aromatic aldehyde complexes $[(\eta^5\text{-}C_5H_5)Re(NO)(PPh_3)(O{=}CHAr)]^+BF_4^-$ (**4a-o**$^+BF_4^-$, 80-97%). IR analyses (CH_2Cl_2, 26 °C) show **4a-o**$^+BF_4^-$ to be >96:<4 to 15:85 mixtures of π/σ isomers (ν_{NO} 1745-1733/1701-1692 cm^{-1}). Electron withdrawing substituents (which enhance aldehyde π acidity and lower σ basicity) favor the π binding mode. Electron donating substituents have an opposite effect. The π/σ ratios increase in more polar solvents and at lower temperatures. Van't Hoff plots give ΔH (**4i,l,o**$^+BF_4^-$; $\pi \rightarrow \sigma$) of 3.6, 2.8, and 1.8 kcal/mol and ΔS of 9.2, 9.5, and 9.1 eu. IR features unique to both binding modes, and visible absorptions characteristic of σ isomers, are identified. Complex **4o**$^+PF_6^-$ crystallizes as a σ isomer, with a conjugated Ar/C=O linkage, a lengthened C=O bond (1.271 (8) Å), and a 0° N-Re-O-C torsion angle. This Re-O conformation maximizes overlap of the d orbital HOMO of the rhenium fragment with C=O π^* orbital lobes on oxygen. The CPMAS ^{13}C NMR spectrum of **4m**$^+BF_4^-$ exhibits a HC=O resonance at 196.2 ppm, consistent with a σ binding mode.

Metal complexes of organic carbonyl compounds play critical roles in a variety of important processes: enzymatic transformations of carboxylic acid derivatives, aldehydes, and ketones;[1,2] biological ion transport;[3] homogeneously and heterogeneously catalyzed reactions of industrial feedstocks;[4] and numerous preparative catalytic transformations.[5] As such, the study of binding between metal fragments and organic carbonyl compounds is of considerable fundamental importance. Notably, diverse types

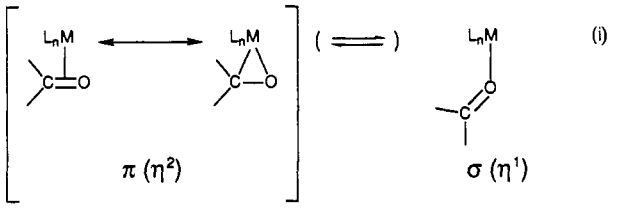

(i)

of isomerism can occur. Of these, the most basic is *linkage* or π/σ (η^2/η^1) isomerism,[6] as illustrated in eq i.

Many π and σ transition-metal aldehyde and ketone complexes have been isolated.[7-9] Surprisingly, however, few quantitative studies of π/σ equilibria have been undertaken.[9,10] Such efforts

(1) (a) Makinen, M. W.; Wells, G. B.; Kang, S.-O. In *Advances in Inorganic Biochemistry*; Eichhorn, G. L., Marzilli, L. G., Eds.; Elsevier: New York, 1984; Vol. 6, Chapter 1. (b) Andrews, R. K.; Blakeley, R. L.; Zerner, B. *Advances in Inorganic Biochemistry*; Eichhorn, G. L., Marzilli, L. G., Eds.; Elsevier: New York, 1984; Chapter 7. (c) Fraüsto da Silva, J. J. R.; Williams, R. J. P. *The Biological Chemistry of the Elements*; Clarendon Press: Oxford, 1991; Chapter 11. (d) Chin, J. *Acc. Chem. Res.* **1991**, *24*, 145. (e) Suh, J. *Acc. Chem. Res.* **1992**, *25*, 273.

(2) (a) MacGibbon, A. K. H.; Koerber, S. C.; Pease, K.; Dunn, M. F. *Biochemistry* **1987**, *26*, 3058. (b) Abriola, D. P.; Fields, R.; Stein, S.; MacKerell, A. D., Jr.; Pietruszko, R. *Biochemistry* **1987**, *26*, 5679. (c) Maret, W.; Zeppezauer, M. *Biochemistry* **1986**, *25*, 1584. (d) Grunwald, J.; Wirz, B.; Scollar, M. P.; Klibanov, A. M. *J. Am. Chem. Soc.* **1986**, *108*, 6732.

(3) Läuger, P. *Angew. Chem., Int. Ed. Engl.* **1985**, *24*, 905.

(4) (a) Nunan, J. G.; Bogdan, C. E.; Klier, K.; Smith, K. J.; Young, C.-W.; Herman, R. G. *J. Catal.* **1988**, *113*, 410. (b) Ishino, M.; Tamura, M.; Deguchi, T.; Nakamura, S. *J. Catal.* **1987**, *105*, 478. (c) Pruett, R. L. *J. Chem. Ed.* **1986**, *63*, 196. (d) Dombek, B. D. *J. Chem. Ed.* **1986**, *63*, 210. (e) Jung, C. W.; Garrou, P. E. *Organometallics* **1982**, *1*, 658.

(5) Representative examples: (a) Chaloner, P. A. *Handbook of Coordination Catalysis in Organic Chemistry*; Butterworths: Boston, 1986; Chapter 7. (b) Brunner, H. *Top. Stereochem.* **1988**, *18*, 129. (c) Bergens, S. H.; Fairlie, D. P.; Bosnich, B. *Organometallics* **1990**, *9*, 566. (d) Bianchini, C.; Meli, A.; Peruzzini, M.; Vizza, F. *J. Am. Chem. Soc.* **1990**, *112*, 6726. (e) Goldman, A. S.; Halpern, J. *J. Organomet. Chem.* **1990**, *382*, 237. (f) Bergens, S. H.; Bosnich, B. *J. Am. Chem. Soc.* **1991**, *113*, 958. (g) Grosselin, J. M.; Mercier, C.; Allmang, G.; Grass, F. *Organometallics* **1991**, *10*, 2126. (h) Menashe, N.; Shvo, Y. *Organometallics* **1991**, *10*, 3885.

(6) Burmeister, J. L. *Coord. Chem. Rev.* **1968**, *3*, 225.

(7) Reviews: (a) Huang, Y.-H.; Gladysz, J. A. *J. Chem. Ed.* **1988**, *65*, 298. (b) Shambayati, S.; Schreiber, S. L. In *Comprehensive Organic Synthesis*; Trost, B. M., Editor-in-Chief; Fleming, I., Deputy Editor-in-Chief; Schreiber, S. L., Volume Editor; Pergamon: New York, 1991; Vol 1, Chapter 1.10.

(8) Lead 1991-1992 references to an extensive literature: (a) Faller, J. W.; Ma, Y. *J. Am. Chem. Soc.* **1991**, *113*, 1579. (b) Faller, J. W.; Ma, Y.; Smart, C. J.; DiVerdi, M. J. *J. Organomet. Chem.* **1991**, *420*, 237. (c) Bullock, R. M.; Rappoli, B. J. *J. Am. Chem. Soc.* **1991**, *113*, 1659. (d) Rabinovich, D.; Parkin, G. *J. Am. Chem. Soc.* **1991**, *113*, 5904. (e) Bachand, B.; Wuest, J. D. *Organometallics* **1991**, *10*, 2015. (f) Adams, H.; Bailey, N. A.; Gauntlett, J. T.; Winter, M. J.; Woodward, S. *J. Chem. Soc., Dalton Trans.* **1991**, 2217. (g) Bochmann, M.; Webb, K. J.; Hursthouse, M. B.; Mazid, M. *J. Chem. Soc., Chem. Commun.* **1991**, 1735. (h) Hill, J. E.; Fanwick, P. E.; Rothwell, I. P. *Organometallics* **1992**, *11*, 1771.

(9) (a) Harman, W. D.; Sekine, M.; Taube, H. *J. Am. Chem. Soc.* **1988**, *110*, 2439. (b) Harman, W. D.; Dobson, J. C.; Taube, H. *J. Am. Chem. Soc.* **1989**, *111*, 3061. (c) Powell, D. W.; Lay, P. A. *Inorg. Chem.* **1992**, *31*, 3542.

(10) Theoretical studies: Delbecq, F.; Sautet, P. *J. Am. Chem. Soc.* **1992**, *114*, 2446.

0002-7863/93/1515-2323$04.00/0

Chart I. Previously Synthesized σ Ketone (2^+X^-) and π Aldehyde (3^+X^-) Complexes of the Rhenium Fragment (I) and Idealized Representations of Preferred Ligand Conformations (II and III)

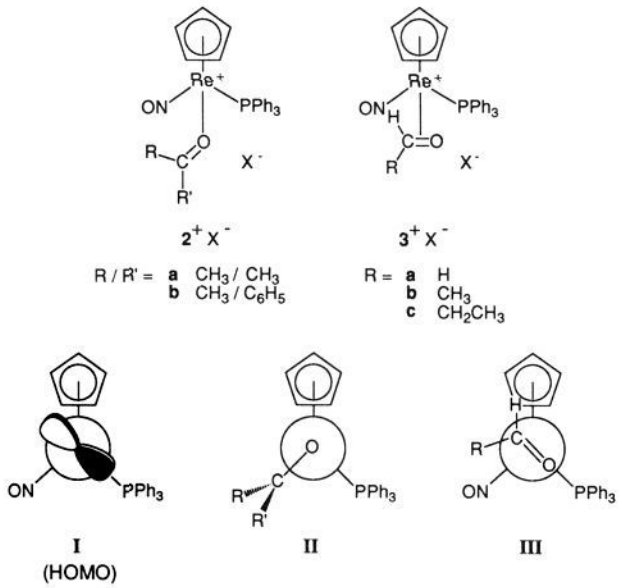

are necessary antecedents to mechanistic investigations aimed at identifying the reactive isomer in a given process. This issue is of particular importance in the context of metal-mediated asymmetric transformations, where enantioselection sometimes originates with the *less* stable of two isomers.[11]

We have previously found that the rhenium dichloromethane complex $[(\eta^5\text{-}C_5H_5)Re(NO)(PPh_3)(ClCH_2Cl)]^+X^-$ ($\mathbf{1}^+X^-$) is readily generated in racemic and optically active forms[12] and reacts with a variety of neutral Lewis bases (L) to give adducts $[(\eta^5\text{-}C_5H_5)Re(NO)(PPh_3)(L)]^+X^-$ in high chemical and optical yields. Thus, $\mathbf{1}^+X^-$ serves as a functional equivalent of the chiral Lewis acid $[(\eta^5\text{-}C_5H_5)Re(NO)(PPh_3)]^+$ (I). The electronic and steric properties of this metal fragment, which is a strong π donor with the high-lying d-orbital HOMO shown in Chart I, have been studied in detail.[13] Hence, I provides a well-defined template for the systematic study of metal/carbonyl group interactions.

In earlier work, we found that $\mathbf{1}^+X^-$ and simple aliphatic and aromatic ketones react to give σ complexes $[(\eta^5\text{-}C_5H_5)Re(NO)(PPh_3)(\eta^1\text{-}O{=}CRR')]^+X^-$ ($\mathbf{2}^+X^-$).[14] No evidence for π isomers was observed. In contrast, analogous reactions of $\mathbf{1}^+X^-$ and *aliphatic* aldehydes gave π complexes $[(\eta^5\text{-}C_5H_5)Re(NO)(PPh_3)(\eta^2\text{-}O{=}CHR)]^+X^-$ ($\mathbf{3}^+X^-$).[15] However, in some cases NMR data suggested small equilibrium concentrations of σ isomers. Crystal structures established that both classes of ligands adopted conformations that allowed a high degree of overlap between the d orbital HOMO of I and the C=O π* acceptor orbital, as illustrated by II and III in Chart I.

We have proposed plausible stereoelectronic rationales for the preceding dichotomy.[14,15] For example, in π isomers both C=O substituents are held in proximity to the metal fragment, whereas in σ isomers only the cis (*Z*) substituent is. Thus, ketones should be sterically less disposed toward π binding than aldehydes. However, a class of ligand was sought for which both binding modes could be simultaneously observed and studied. In this paper, we report (1) the synthesis of 15 aromatic aldehyde complexes of the formula $[(\eta^5\text{-}C_5H_5)Re(NO)(PPh_3)(O{=}CHAr)]^+X^-$ ($\mathbf{4}^+X^-$), which exist as varying mixtures of π/σ isomers, (2) the measurement of K_{eq}, ΔH, and ΔS for π/σ binding, (3) the detailed spectroscopic characterization of $\mathbf{4}^+X^-$, with emphasis upon IR and UV visible features unique to each binding mode, (4) crystallographic and CPMAS ^{13}C NMR studies of representative σ complexes, and (5) analyses of substituent, solvent, and temperature effects upon K_{eq}. Portions of this study, and a companion effort with α-halogenated ketones, have been communicated.[16,17]

Scheme I. Synthesis of and IR Data for Aromatic Aldehyde Complexes $[(\eta^5\text{-}C_5H_5)Re(NO)(PPh_3)(O{=}CHAr)]^+BF_4^-$ ($4^+BF_4^-$)

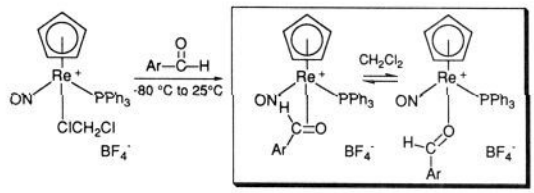

	Complex	IR ν_{NO} [a] π	IR ν_{NO} [a] σ	π/σ [c] Ratio	K_{eq} [d]	ΔG (cal/mol)
Ar =	a. C_6F_5	1745	b	>96:<4	-	-
	b. 4-$C_6H_4CF_3$	1742	b	>96:<4	-	-
	c. 3-$C_6H_4CF_3$	1741	b	>96:<4	-	-
	d. 3-$C_6H_4OCH_3$	1739	1701	90:10	0.11	1301
	e. 2-$C_6H_4OCH_3$	1739	1700	89:11	0.12	1241
	f. 4-C_6H_4Cl	1740	1701	83:17	0.20	960
	g. 4-C_6H_4F	1739	1701	83:17	0.21	925
	h. 1-naphthyl	1741	1700	82:18	0.23	881
	i. C_6H_5	1739	1702	84:16	0.20	972
	j. 3,4,5-$C_6H_2(OCH_3)_3$	1735	1697	64:36	0.56	350
	k. 4-$C_6H_4C_6H_5$	1739	1700	64:36	0.57	334
	l. 4-$C_6H_4CH_3$	1738	1699	53:47	0.87	86
	m. 2,4-$C_6H_3(OCH_3)_2$	1736	1692	25:75	3.07	-665
	n. 3,4-$C_6H_3(OCH_3)_2$	1733	1694	24:76	3.16	-682
	o. 4-$C_6H_4OCH_3$	1735	1693	15:85	5.87	-1050

[a] In CH_2Cl_2 at 26 °C. [b] No absorption observed; detection limit < 4%. [c] We assign error limits of ± 2 to each component of the normalized π/σ ratios; e.g., 84:16 = (84 ± 2):(16 ± 2). [d] Due to roundoff protocols, compounds with identical π/σ isomer ratios can give different K_{eq}.

Results

1. Synthesis of Title Complexes. The methyl complex $(\eta^5\text{-}C_5H_5)Re(NO)(PPh_3)(CH_3)$ (**5**)[18] and $HBF_4{\cdot}OEt_2$ were reacted in CH_2Cl_2 at −80 °C as previously described to give the dichloromethane complex $[(\eta^5\text{-}C_5H_5)Re(NO)(PPh_3)(ClCH_2Cl)]^+BF_4^-$ ($\mathbf{1}^+BF_4^-$).[12] Then aromatic aldehydes ArC-H=O (**6a–o**, 2–3 equiv) were added. Workup gave the substitution products $[(\eta^5\text{-}C_5H_5)Re(NO)(PPh_3)(O{=}CHAr)]^+BF_4^-$ (**4a–o**$^+BF_4^-$) in 80–97% yields as spectroscopically pure powders (Scheme I). These either gave correct microanalyses or could be crystallized to samples that did. The parent benzaldehyde complex **4i**$^+BF_4^-$ has been reported earlier.[15a]

Complexes $\mathbf{4}^+BF_4^-$ were characterized by IR and NMR (^1H, ^{13}C, ^{31}P) spectroscopy. Data acquired at room temperature are summarized in Scheme I and Table I. Divergent NMR properties were evident. Some complexes exhibited C=O ^{13}C NMR and PPh_3 ^{31}P NMR chemical shifts similar to those of π-aldehyde complexes $\mathbf{3}^+X^-$ (60–90 and 9–11 ppm).[15] Several gave C=O ^{13}C NMR and PPh_3 ^{31}P NMR chemical shifts closer to those of σ ketone complexes $\mathbf{2}^+X^-$ (216–240 and 18–19 ppm).[14] Others exhibited intermediate properties. Similar trends were found for the HC=O and cyclopentadienyl ^1H NMR chemical shifts (δ 5.2–5.4 and 5.8–5.9 in $\mathbf{3}^+X^-$). Selected data are represented

(11) (a) McCulloch, B.; Halpern, J.; Thompson, M. R.; Landis, C. R. *Organometallics* **1990**, *9*, 1392. (b) Bogdan, P. L.; Irwin, J. J.; Bosnich, B. *Organometallics* **1989**, *8*, 1450.

(12) Fernández, J. M.; Gladysz, J. A. *Organometallics* **1989**, *8*, 207.

(13) (a) Schilling, B. E. R.; Hoffmann, R.; Faller, J. W. *J. Am. Chem. Soc.* **1979**, *101*, 592. (b) Kiel, W. A.; Lin, G.-Y.; Constable, A. G.; McCormick, F. B.; Strouse, C. E.; Eisenstein, O.; Gladysz, J. A. *J. Am. Chem. Soc.* **1982**, *104*, 4865. (c) Georgiou, S.; Gladysz, J. A. *Tetrahedron* **1986**, *42*, 1109. (d) Czech, P. T.; Gladysz, J. A.; Fenske, R. F. *Organometallics* **1989**, *8*, 1806. (e) Lichtenberger, D. L.; Rai-Chaudhuri, A. R.; Seidel, M. J.; Gladysz, J. A.; Agbossou, S. K.; Igau, A.; Winter, C. H. *Organometallics* **1991**, *10*, 1355.

(14) (a) Dalton, D. M.; Fernández, J. M.; Emerson, K.; Larsen, R. D.; Arif, A. M.; Gladysz, J. A. *J. Am. Chem. Soc.* **1990**, *112*, 9198. (b) Dalton, D. M.; Gladysz, J. A. *J. Chem. Soc., Dalton Trans.* **1991**, 2741.

(15) (a) Garner, C. M.; Quirós Méndez, N.; Kowalczyk, J. M.; Fernández, J. M.; Emerson, K.; Larsen, R. D.; Gladysz, J. A. *J. Am. Chem. Soc.* **1990**, *112*, 5146. (b) Klein, D. P.; Quirós Méndez, N.; Seyler, J. W.; Arif, A. M.; Gladysz, J. A. *J. Organomet. Chem.*, in press.

(16) Quirós Méndez, N.; Arif, A. M.; Gladysz, J. A. *Angew. Chem., Int. Ed. Engl.* **1990**, *29*, 1473.

(17) Klein, D. P.; Dalton, D. M.; Quirós Méndez, N.; Arif, A. M.; Gladysz, J. A. *J. Organomet. Chem.* **1991**, *412*, C7.

(18) Tam, W.; Lin, G.-Y.; Wong, W.-K.; Kiel, W. A.; Wong, V. K.; Gladysz, J. A. *J. Am. Chem. Soc.* **1982**, *104*, 141.

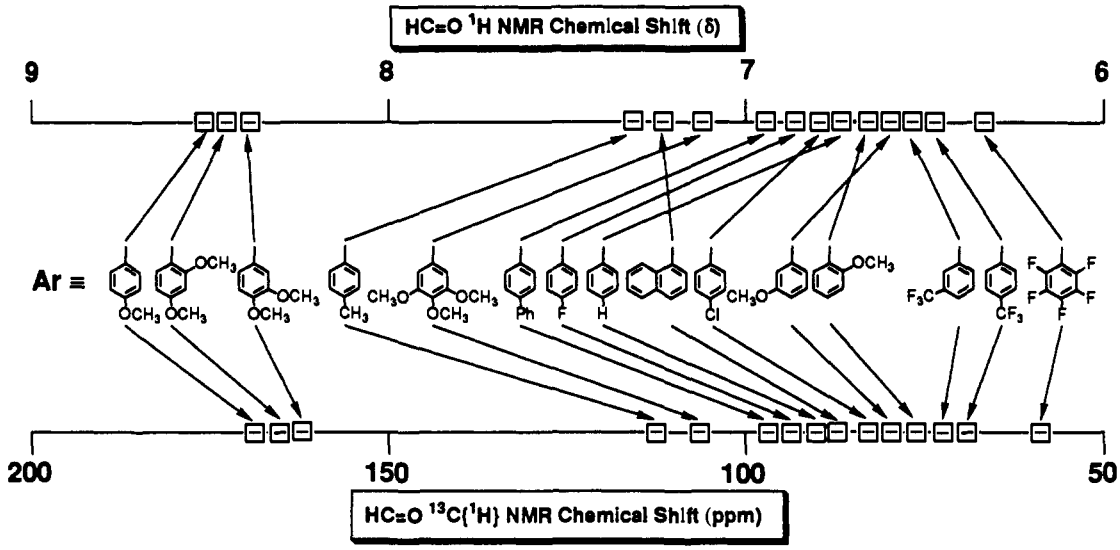

Figure 1. Trends in ^{1}H NMR and ^{13}C NMR HC=O chemical shifts in aromatic aldehyde complexes $[(\eta^5\text{-}C_5H_5)Re(NO)(PPh_3)(O{=}CHAr)]^+BF_4^-$ ($\mathbf{4}^+BF_4^-$); for exact values and temperatures, see Table I.

pictorially in Figure 1. These observations suggest that $\mathbf{4}^+BF_4^-$ exist as rapidly equilibrating, varying mixtures of π/σ isomers. The IR data are analyzed below.

Derivatives of $\mathbf{4}^+BF_4^-$ were sought for spectroscopic experiments. First, $\mathbf{1}^+BF_4^-$ and monodeuterated *p*-methoxybenzaldehyde, 4-$CH_3OC_6H_4(C{=}O)D$, were reacted to give the corresponding labeled complex $\mathbf{4o}^+\text{-}d_1\,BF_4^-$. Second, the optically active methyl complex (+)-(*S*)-**5** was converted to the dichloromethane complex (*S*)-$\mathbf{1}^+BF_4^-$.[12] Subsequent reaction with the labeled benzaldehyde $C_6H_5(^{13}C{=}O)H$ gave the corresponding optically active complex (+)-(*RS*)-$\mathbf{4i}^+\text{-}^{13}CBF_4^-$.[19] This compound is considerably more soluble than the racemate, which facilitates measurements described below.

Selected hexafluorophosphate salts were also desired. However, $HPF_6{\cdot}OEt_2$, which is required to generate the precursor dichloromethane complex $\mathbf{1}^+PF_6^-$, is no longer commercially available in sufficiently pure form. Thus, a protocol utilized to prepare the cationic alcohol complexes $[(\eta^5\text{-}C_5H_5)Re(NO)(PPh_3)(ROH)]^+PF_6^-$ was employed.[20] First, the hydride complex $(\eta^5\text{-}C_5H_5)Re(NO)(PPh_3)(H)$ (**7**)[21] and $Ph_3C^+PF_6^-$ were combined in CH_2Cl_2 at −80 °C. Then the aldehydes **6b,i,o** were added. Workup gave $\mathbf{4b,i,o}^+PF_6^-$ in 76–88% yields. Analogous reactions with labeled aldehydes $C_6H_5(^{13}C{=}O)H$ and 4-$CH_3OC_6H_4(C{=}O)D$ gave the corresponding labeled complexes $\mathbf{4i}^+\text{-}^{13}CPF_6^-$ and $\mathbf{4o}^+\text{-}d_1\,PF_6^-$. Recently, procedures for metathesizing $\mathbf{3,4}^+BF_4^-$ to $\mathbf{3,4}^+PF_6^-$ have also been developed.[15b]

2. Room Temperature IR Spectra. (A) Analysis of ν_{NO}. The σ ketone complexes $\mathbf{2}^+X^-$ exhibit IR ν_{NO} of 1697–1680 cm^{-1},[14] whereas the aliphatic π aldehyde complexes $\mathbf{3}^+X^-$ give IR ν_{NO} of 1740–1729 cm^{-1}.[15] Thus, backbonding into the nitrosyl ligand is greater in the σ ketone complexes $\mathbf{2}^+X^-$. This implies that π aldehyde ligands are weaker σ donors and/or stronger π acceptors than σ ketone ligands.[22] The σ donor trend follows from the relative energies of C=O σ and π orbitals. The π acceptor trend is expected from the lower C=O π^* orbital energies of aldehydes.[7a,10] Also, overlap between the HOMO of the rhenium fragment **I** (Chart I) and the C=O π^* orbital is restricted to only the =O lobes in the σ binding mode.

The aromatic aldehyde complexes $\mathbf{4}^+BF_4^-$ exhibited differing IR ν_{NO} properties (Scheme I). Some ($\mathbf{4a\text{–}c}^+BF_4^-$) gave a single absorption in the region of π complexes $\mathbf{3}^+X^-$. Others ($\mathbf{4d\text{–}o}^+BF_4^-$) showed *two* absorptions—one in the range of π complexes $\mathbf{3}^+X^-$,

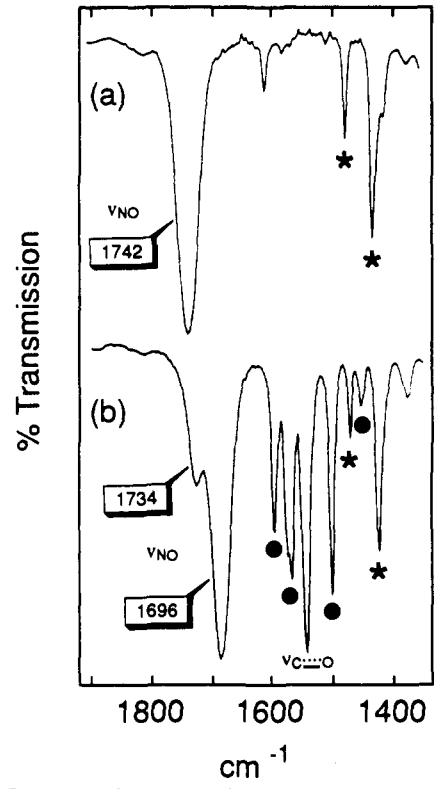

Figure 2. IR spectra of representative aldehyde complexes: (a) *p*-trifluoromethylbenzaldehyde complex $\mathbf{4b}^+BF_4^-$ and (b) *p*-methoxybenzaldehyde complex $\mathbf{4o}^+BF_4^-$. The absorptions designated with * and • are associated with the PPh_3 and aldehyde aryl moieties as described in the text.

and the other in the range of σ complexes $\mathbf{2}^+X^-$. Hence, these were assigned to π and σ isomers. Additional supporting evidence is given below. Representative spectra are shown in Figure 2, and others are published elsewhere.[16,23]

The IR ν_{NO} absorptions of π and σ reference compounds were quantified. An IR spectrum was recorded of a CH_2Cl_2 solution that was 0.01 M in both the π formaldehyde complex $[(\eta^5\text{-}C_5H_5)Re(NO)(PPh_3)(\eta^2\text{-}O{=}CH_2)]^+BF_4^-$ ($\mathbf{3a}^+BF_4^-$)[24] *and* σ

(19) The absolute configurations of the rhenium and carbon stereocenters are specified as described previously.[15a]
(20) Agbossou, S. K.; Smith, W. W.; Gladysz, J. A. *Chem. Ber.* **1990**, *123*, 1293.
(21) Crocco, G. L.; Gladysz, J. A. *J. Am. Chem. Soc.* **1988**, *110*, 6110.
(22) Bursten, B. E.; Green, M. R. *Prog. Inorg. Chem.* **1988**, *36*, 393.
(23) N. Quirós Méndez, Ph.D. Thesis, University of Utah, 1991.
(24) (a) Buhro, W. E.; Georgiou, S.; Fernández, J. M.; Patton, A. T.; Strouse, C. E.; Gladysz, J. A. *Organometallics* **1986**, *5*, 956. (b) The tetrafluoroborate salt $\mathbf{3a}^+BF_4^-$ is prepared by a procedure analogous to that reported for $\mathbf{3a}^+PF_6^-$.

Table I. NMR Characterization of Aromatic Aldehyde Complexes $[(\eta^5\text{-}C_5H_5)Re(NO)(PPh_3)(O{=}CHAr)]^+BF_4^-$ ($\mathbf{4}^+BF_4^-$)

complex (Ar)	^1H NMR[a] (δ)	$^{13}C\{^1H\}$ NMR[b] (ppm)	$^{31}P\{^1H\}$ NMR[c] (ppm)
4a$^+BF_4^-$ (C_6F_5)	7.69–7.45 (m, $3C_6H_5$), 6.35 (d, J_{HP} = 1.4, HCO), 6.18 (br s, C_5H_5)	PPh_3 at 133.8 (d, J = 10.4, *o*), 133.4 (d, J = 2.9, *p*), 130.1 (d, J = 11.7, *m*), 126.9 (d, J = 60.7, *i*) CAr at[d,e] 144.8 (dm, $^1J_{CF}$ = 264.5), 137.8 (dm, $^1J_{CF}$ = 264.4), 115.9 (m); 100.5 (s, C_5H_5), 62.8 (s, CO), 24.6 (s, CH_3)	9.88 (s)
4b$^+BF_4^-$ (4-$C_6H_4CF_3$)	7.72–7.42 (m, $3C_6H_5$ and 2 H of C_6H_4), 7.04 (br s, 2 H of C_6H_4), 6.54 (br s, HCO), 6.03 (br s, C_5H_5)	PPh_3 at 134.0 (d, J = 10.3, *o*), 133.3 (d, J = 2.8, *p*), 130.0 (d, J = 11.5, *m*), 127.5 (d, J = 60.1, *i*) CAr at[e] 144.3 (s), 130.7 (d, $^2J_{CF}$ = 37.8), 126.9 (br s), 125.4 (d, $^3J_{CF}$ = 3.3); 124.0 (q, $^1J_{CF}$ = 272.1, CF_3), 100.0 (s, C_5H_5), 74.9 (s, CO)	9.46 (s)
4c$^+BF_4^-$ (3-$C_6H_4CF_3$)	7.72–7.42 (m, $3C_6H_5$), 7.53–7.35 (m, 3 H of C_6H_4), 7.08 (br s, 1 H of C_6H_4), 6.57 (d, J_{HP} = 2.0, HCO), 6.03 (br s, C_5H_5)	PPh_3 at 133.8 (d, J = 10.2, *o*), 133.1 (d, J = 2.9, *p*), 129.9 (d, J = 11.7, *m*), 127.4 (d, J = 59.8, *i*) CAr at[d,e] 141.6 (s), 131.1 (br s), 129.2 (s), 126.1 (d, J_{CF} = 3.8), 122.0 (br s); 99.9 (s, C_5H_5), 76.1 (s, CO)[f]	9.68 (s)
4d$^+BF_4^-$ (3-$C_6H_4OCH_3$)	7.70–7.49 (m, $3C_6H_5$), 7.25 (pseudo t, J = 8.1, 1 H of C_6H_4), 6.78 (d, J = 8.3, 1 H of C_6H_4), 6.65 (d, J = 7.6, 1 H of C_6H_4), 6.64 (s, 1 H of C_6H_4), 6.63 (br s, HCO), 5.90 (s, C_5H_5), 3.71 (s, OCH_3)	PPh_3 at 134.0 (d, J = 10.3, *o*), 133.1 (d, J = 2.9, *p*), 130.0 (d, J = 11.8, *m*), 128.0 (d, J = 58.7, *i*) CAr at 159.1 (s, C=*C*—O), 131.9 (s), 128.1 (s), 124.8 (s), 120.1 (s), 110.7 (s); 98.9 (s, C_5H_5), 82.1 (br s, CO), 56.2 (s, OCH_3)	10.45 (s)
4e$^+BF_4^-$ (2-$C_6H_4OCH_3$)	7.69–7.48 (m, $3C_6H_5$), 7.17 (pseudo t, J = 8.6, 1 H of C_6H_4), 6.98 (d, J = 7.8, 1 H of C_6H_4), 6.81 (pseudo t, J = 7.6, 1 H of C_6H_4), 6.64 (d, J_{HP} = 1.9, HCO), 6.54 (d, J = 7.7, 1 H of C_6H_4), 5.98 (s, C_5H_5), 4.02 (s, OCH_3)	PPh_3 at 133.9 (d, J = 10.5, *o*), 133.0 (d, J = 2.8, *p*), 129.9 (d, J = 11.5, *m*), 127.8 (d, J = 59.4, *i*) CAr at 158.9 (s, C=*C*—O), 131.7 (s), 128.0 (s), 124.5 (s), 119.9 (s), 110.5 (s); 98.9 (s, C_5H_5), 80.4 (br s, CO), 56.0 (s, OCH_3)	11.50 (s)
4f$^+BF_4^-$ (4-C_6H_4Cl)	7.70–7.52 (m, $3C_6H_5$), 7.28 (d, J = 8.5, 2 H of C_6H_4), 6.93 (d, J = 8.5, 2 H of C_6H_4), 6.82 (d, J_{HP} = 1.9, HCO), 5.96 (s, C_5H_5)	PPh_3 at 134.0 (d, J = 10.8, *o*), 133.3 (s, *p*), 130.1 (d, J = 11.0, *m*), 127.8 (d, J = 56.5, *i*) CAr at 138.5 (s), 136.1 (s), 128.9 (s), 128.4 (s); 99.6 (s, C_5H_5), 83.4 (br s, CO)	9.81 (s)
4g$^+BF_4^-$ (4-C_6H_4F)	7.68–7.49 (m, $3C_6H_5$), 7.08–6.97 (m, C_6H_4), 6.93 (d, J_{HP} = 1.8, HCO), 5.93 (s, C_5H_5)	PPh_3 at 134.0 (d, J = 10.8, *o*), 133.1 (d, J = 3.1, *p*), 130.0 (d, J = 11.4, *m*), 128.0 (d, J = 59.5, *i*) CAr at[e] 164.1 (d, $^1J_{CF}$ = 250.8), 135.9 (d, $^4J_{CF}$ = 3.0), 129.4 (d, $^3J_{CF}$ = 8.0), 115.7 (d, $^2J_{CF}$ = 22.0); 99.2 (s, C_5H_5), 90.0 (br s, CO)	10.55 (s)
4h$^+BF_4^-$ (1-naphthyl)	8.35 (d, J = 8.3, 1 H of $C_{10}H_7$), 7.91 (d, J = 8.1, 1 H of $C_{10}H_7$), 7.81–7.44 (m, $3C_6H_5$ and 3 H of $C_{10}H_7$), 7.35 (pseudo t, J = 7.7, 1 H of $C_{10}H_7$), 7.17 (br s, HCO), 6.79 (d, J = 6.9, 1 H of $C_{10}H_7$), 5.77 (s, C_5H_5)	PPh_3 at 133.9 (d, J = 10.6, *o*), 133.2 (s, *p*), 130.1 (d, J = 11.7, *m*), 127.8 (d, J = 59.8, *i*) CAr at[d] 134.9 (s), 133.6 (s), 131.7 (s), 131.0 (s), 129.8 (s), 128.4 (s), 126.9 (s), 125.0 (s), 122.1 (s); 99.8 (s, C_5H_5), 85.0 (br s, CO)	11.37 (s)
4i$^+BF_4^-$ (C_6H_5)	6.81 (d, J_{HP} = 1.4, HCO), 5.89 (s, C_5H_5)[g]	99.3 (s, C_5H_5), 89.5 (br s, CO)[g]	10.05 (s)
4j$^+BF_4^-$ (3,4,5-$C_6H_2(OCH_3)_3$)	7.64–7.47 (m, $3C_6H_5$), 7.10 (d, J_{HP} = 1.4, HCO), 6.47 (s, 2 H of C_6H_2), 5.87 (s, C_5H_5), 3.78 (s, OCH_3), 3.72 (s, 2OCH_3)	PPh_3 at 133.9 (d, J = 10.4, *o*), 132.8 (d, J = 2.5, *p*), 129.9 (d, J = 11.2, *m*), 128.5 (d, J = 58.5, *i*) CAr at 153.4 (s, C=*C*—O), 141.8 (s, C=*C*—O), 134.0 (s), 105.2 (s); 109.7 (br s, CO), 98.3 (s, C_5H_5), 61.3 (s, OCH_3), 56.5 (s, 2OCH_3)	11.91 (s)
4k$^+BF_4^-$ (4-$C_6H_4C_6H_5$)	7.85–7.23 (m, $3C_6H_5$ and 7 H of $C_{10}H_9$), 7.15 (d, J = 8.3, 2 H of $C_{10}H_9$), 6.98 (br s, HCO), 5.90 (s, C_5H_5)	PPh_3 at 133.8 (d, J = 10.0, *o*), 132.9 (d, J = 3.0, *p*), 129.8 (d, J = 11.4, *m*), 127.8 (d, J = 53.7, *i*) CAr at 143.2 (s), 139.6 (s), 138.2 (s), 129.0 (s), 128.2 (s), 127.7 (s), 127.3 (s), 127.0 (s); 98.9 (s, C_5H_5), 92.6 (br s, CO)	11.28 (s)
4l$^+BF_4^-$ (4-$C_6H_4CH_3$)	7.67–7.45 (m, $3C_6H_5$), 7.29 (br s, HCO), 7.20 (d, J = 8.1, 2 H of C_6H_4), 7.05 (d, J = 8.2, 2 H of C_6H_4), 5.83 (s, C_5H_5), 2.46 (s, CH_3)	PPh_3 at 134.0 (d, J = 10.6, *o*), 132.9 (*s*, *p*), 130.0 (d, J = 11.2, *m*), 128.9 (d, *i*)[d] CAr at 143.4 (s), 135.6 (s), 129.6 (s), 128.2 (s); 113.6 (br s, CO), 98.1 (s, C_5H_5), 21.5 (s, CH_3)	12.85 (s)
4m$^+BF_4^-$ (2,4-$C_6H_3(OCH_3)_2$)	8.63 (s, HCO), 7.55–7.47 (m, 9 H of $3C_6H_5$), 7.41–7.32 (m, 6 H of $3C_6H_5$), 7.06 (d, J = 8.8, 1 H of C_6H_3), 6.49 (ddd, J = 9.0, 2.2, 0.7, 1 H of C_6H_3), 6.43 (d, J = 2.2, 1 H of C_6H_3), 5.72 (s, C_5H_5), 3.93 (s, OCH_3), 3.91 (s, OCH_3)	PPh, at 133.9 (d, J = 10.9, *o*), 133.2 (d, J = 2.6, *p*), 130.1 (d, J = 56.5, *i*), 129.7 (d, J = 11.0, *m*) CAr at 168.6 (s, C=*C*—O), 164.0 (s, C=*C*—O), 131.2 (s), 118.6 (s), 107.8 (s), 97.3 (s); 166.2 (br s, CO), 94.6 (s, C_5H_5), 56.5 (s, OCH_3), 56.4 (s, OCH_3)	17.78 (s)

Table I (Continued)

complex (Ar)	^{1}H NMR[a] (δ)	^{13}C{^{1}H} NMR[b] (ppm)	^{31}P{^{1}H} NMR[c] (ppm)
4n$^+$$BF_4^-$ (3,4-$C_6H_3(OCH_3)_2$)	8.31 (s, HCO), 7.57–7.48 (m, 9 H of $3C_6H_5$), 7.43–7.36 (m, 6 H of $3C_6H_5$), 7.03 (dd, J = 8.4, 2.0, 1 H of C_6H_3), 6.91 (d, J = 8.5, 1 H of C_6H_3), 6.84 (d, J = 1.9, 1 H of C_6H_3), 5.76 (s, C_5H_5), 3.91 (s, OCH_3), 3.79 (s, OCH_3)	PPh_3 at 133.9 (d, J = 10.8, *o*), 132.3 (d, J = 2.5, *p*), 129.9 (d, J = 56.4, *i*), 129.8 (d, J = 10.9, *m*) CAr at 156.3 (s, C=*C*—O), 149.7 (s, (C=*C*—O), 129.4 (s), 127.5 (s), 110.9 (s), 110.2 (s); 165.5 (br s, CO), 95.1 (s, C_5H_5), 56.6 (s, OCH_3), 56.4 (s, OCH_3)	17.05 (s)
4o$^+$$BF_4^-$ (4-$C_6H_4OCH_3$)	8.42 (s, HCO), 7.54–7.49 (m, 9 H of $3C_6H_5$), 7.41–7.32 (m, 6 H of $3C_6H_5$ and 2 H of C_6H_4), 6.93 (d, J = 8.9, 2 H of C_6H_4), 5.74 (s, C_5H_5), 3.89 (s, OCH_3)	PPh_3 at 133.9 (d, J = 10.7, *o*), 133.3 (d, J = 2.5, *p*), 129.8 (d, J = 11.0, *m*), 129.8 (d, J = 56.6, *i*) CAr at 166.2 (s, C=*C*—O), 133.0 (s), 129.0 (s), 114.8 (s); 169.1 (br s, CO), 94.9 (s, C_5H_5), 56.3 (s, OCH_3)	17.73 (s)

[a] Recorded at 300 MHz in CD_2Cl_2 at ambient probe temperature and referenced to internal $Si(CH_3)_4$. All coupling constants are in Hz and to ^{1}H unless noted. [b] Recorded at 75 MHz in CD_2Cl_2 at ambient probe temperature and referenced to CD_2Cl_2 (53.8 ppm). All couplings are in Hz and to ^{31}P unless noted. Phenyl resonances are assigned as described in footnote c of Table I in ref 24a. [c] Recorded at 121 MHz in CD_2Cl_2 at ambient probe temperature and referenced to external 85% H_3PO_4. [d] One CAr or PPh_3 resonance is entirely or partially obscured. [e] The J_{CF} are assigned as previously described: Weigert, F. J.; Roberts, J. D. *J. Am. Chem. Soc.* **1969**, *91*, 4940. [f] The CF_3 resonance is not observed. [g] Complete data are given in ref 15a.

acetone complex $[(\eta^5\text{-}C_5H_5)Re(NO)(PPh_3)(\eta^1\text{-}O{=}C(CH_3)_2)]^+\text{-}BF_4^-$ (**2a**$^+$$BF_4^-$).[14a] The areas of the ν_{NO} bands (1745, 1696 cm^{-1}) were identical within 0.3%. Thus, area ratios were used to calculate all equilibrium constants given below. The intensities of the π and σ ν_{NO} absorptions differed somewhat at λ_{max}. Consequently, the molar extinction coefficients were unequal (ϵ = 352, 430 M^{-1}cm^{-1}).

Next, the relative areas of the π and σ IR ν_{NO} absorptions of **4**$^+$$BF_4^-$ were measured in CH_2Cl_2 at 26 °C (Experimental Section). The data, summarized in Scheme I, gave K_{eq} ($\pi \rightarrow \sigma$) that ranged from <0.04 for pentafluorobenzaldehyde complex **4a**$^+$$BF_4^-$ to 5.67 for *p*-methoxybenzaldehyde complex **4o**$^+$$BF_4^-$. Similarly, $\Delta G_{299\ K}$ ranged from >2.0 to −1.05 kcal/mol. Aldehyde ligands with electron donating arene substituents generally gave greater proportions of σ isomers, whereas those with electron withdrawing substituents favored π isomers.

(B) Other IR Features of σ Isomers. We sought to identify IR absorptions characteristic of σ isomers of **4**$^+$$BF_4^-$. For example, free aldehydes exhibit a C–H bending vibration (δ_{CH}) near 1390 cm^{-1} and a C–H stretching vibration (ν_{CH}) at 2700–2850 cm^{-1}.[25] The latter is often a doublet. Hence, IR spectra of uncoordinated *p*-methoxybenzaldehyde (**6o**), and the predominantly σ complexes **4o**$^+$$BF_4^-$ and **4o**$^+$-$d_1BF_4^-$, were compared. First, **6o** exhibited the expected δ_{CH} (1394 cm^{-1} w) and ν_{CH} (2740/2806 cm^{-1} w) absorptions. Subtraction of the IR spectrum of **4o**$^+$-$d_1BF_4^-$ from that of **4o**$^+$$BF_4^-$ revealed a δ_{CH} band at 1389 cm^{-1}. The corresponding δ_{CD} band was tentatively assigned to a shoulder at 1034 cm^{-1}. However, both spectra were identical between 2500 and 3200 cm^{-1}. Thus, a ν_{CH} absorption could not be assigned.

The IR spectrum of **4o**$^+$$BF_4^-$ was next compared to that of the predominantly π complex **4b**$^+$$BF_4^-$ (Figure 2). Absorptions at 1483–1482 and 1437–1435 cm^{-1} (labeled *) appeared in both. These have been found in all compounds of the formula $[(\eta^5\text{-}C_5H_5)Re(NO)(PPh_3)(L)]^{n+}$ and were attributed to the PPh_3 ligand (free PPh_3: 1485, 1438 cm^{-1}).[26a] Four IR bands of **4o**$^+$$BF_4^-$ (1607, 1580, 1512, 1464 cm^{-1}; labeled ·) had close analogy in the spectrum of *p*-methoxybenzaldehyde **6o** (1601, 1578, 1511, 1460 cm^{-1}, thin film) and were assigned as aryl ν_{C-C} absorptions. Such absorptions have been shown to be much more intense when the arene ring is substituted with electron donating groups.[26b] Thus, they should be greatly diminished in IR spectra of π complexes such as **4b**$^+$$BF_4^-$.

The more intense 1555 cm^{-1} IR absorption of **4o**$^+$$BF_4^-$ was assigned as the $\nu_{C=O}$. Hence, the IR $\nu_{C=O}$ of **6o** (1687 cm^{-1}) decreases by 132 cm^{-1} upon coordination to the rhenium fragment I. The $\nu_{C=O}$ of **4o**$^+$$BF_4^-$ is lower than those of the corresponding *aliphatic* σ ketone complexes (1605–1625 cm^{-1}), such as the acetone adduct **2a**$^+$$BF_4^-$ (Chart I).[14] However, it matches that of an *aromatic* σ ketone complex, acetophenone adduct **2b**$^+$$BF_4^-$. As expected,[26b] the $\nu_{C=O}$ and ν_{C-C} absorptions of **4o**$^+$$BF_4^-$ are more intense than those of **2b**$^+$$BF_4^-$ (vs ν_{NO} as reference).

(C) Other IR Features of π Isomers. We sought to identify IR absorptions characteristic of π isomers of **4**$^+$$BF_4^-$. Thus, spectra of the benzaldehyde complex **4i**$^+$$BF_4^-$ and the optically active ^{13}C-labeled analog, (+)-(*RS*)-**4i**$^+$-^{13}CBF_4^-, were compared. Since the 960–1130-cm^{-1} region is obscured by the tetrafluoroborate anion, spectra of racemic **4i**$^+$$PF_6^-$ and **4i**$^+$-^{13}CPF_6^- were also recorded. The hexafluorophosphate anion in turn obscures the 800-900-cm^{-1} region.

Three weak bands in the unlabeled complexes **4i**$^+$$X^-$ (1258/1263 (BF_4^-/PF_6^-), 1007 (PF_6^-), 820 (BF_4^-) cm^{-1}) shifted in the ^{13}C derivatives (1236/1250, 990, 803 cm^{-1}). In order to help interpret these absorptions, the IR spectra of hydride complex $(\eta^5\text{-}C_5H_5)Re(NO)(PPh_3)(H)$ (**7**; ν_{ReH} 1957 cm^{-1} m),[21] methyl complex $(\eta^5\text{-}C_5H_5)Re(NO)(PPh_3)(CH_3)$ (**5**),[18] and methoxide complex $(\eta^5\text{-}C_5H_5)Re(NO)(PPh_3)(OCH_3)$[24a] were carefully compared. The methyl complex exhibited a unique band at 1211 cm^{-1} (w). The methoxide complex gave unique bands at 1050 (ν_{C-O} m), 903 (w), and 793 (w) cm^{-1}. Hence, one possibility would be to assign the 1007 cm^{-1} absorption of **4i**$^+$$X^-$ as the ν_{C-O}, and the 1258/1263 and 820 cm^{-1} bands to other vibrational modes associated with the aldehyde ligand carbon.

Other researchers have assigned IR ν_{C-O} in π aldehyde and ketone complexes, sometimes by use of isotopically labeled substrates.[7a,27] In general, medium-intensity absorptions are found at 1000–1300 cm^{-1}. However, in most cases only *one* isotopically shifted band has been reported, as opposed to the three of **4i**$^+$$X^-$. Interestingly, organic epoxides exhibit three diagnostic IR absorptions at 1250, 950–810, and 840–750 cm^{-1}—commonly referred to as "8μ", "11μ", and "12μ" bands.[28] This striking parallel suggests that the IR properties of π isomers of **4**$^+$$X^-$ are best analyzed in the context of the metallacyclic resonance form **B** (eq i).

3. Temperature and Solvent Dependence of π/σ Equilibria. Variable temperature IR spectra of benzaldehyde complex **4i**$^+$-

(25) Silverstein, R. M.; Bassler, G. C.; Morrill, T. C. *Spectrometric Identification of Organic Compounds*, 5th ed.; Wiley: New York, 1991; p 117.

(26) (a) Pouchert, C. J. *The Aldrich Library of Infrared Spectra*; Aldrich Chemical Co.: Milwaukee, WI, 1981; p 1182A. (b) Pouchert, C. J. *The Aldrich Library of Infrared Spectra*; Aldrich Chemical Co.: Milwaukee, WI, 1981; pp 913C, 914H.

(27) (a) Bryan, J. C.; Mayer, J. M. *J. Am. Chem. Soc.* **1990**, *112*, 2298. (b) Wood, C. D.; Schrock, R. R. *J. Am. Chem. Soc.* **1979**, *101*, 5421. (c) Harman, W. D.; Fairlie, D. P.; Taube, H. *J. Am. Chem. Soc.* **1986**, *108*, 8223.

(28) Nakanishi, K. *Infrared Absorption Spectroscopy*; Holden-Day: San Francisco, 1962; p 36.

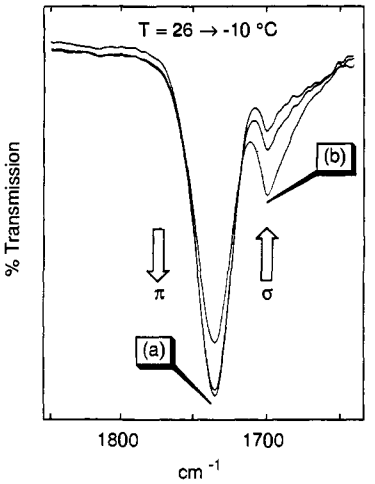

Figure 3. Representative variable temperature IR spectra. Benzaldehyde complex (+)-(*RS*)-**4i**$^+$$BF_4^-$ in CH_2Cl_2 at 26, 0, and −10 °C: (a) ν_{NO} of π isomer and (b) ν_{NO} of σ isomer.

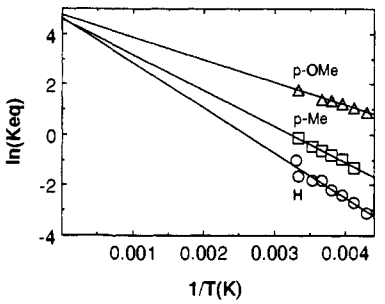

Figure 4. van't Hoff plots for the temperature-dependent π/σ equilibria of aromatic aldehyde complexes **4i,l,o**$^+$$BF_4^-$.

BF_4^-, *p*-methylbenzaldehyde complex **4l**$^+$$BF_4^-$, and *p*-methoxybenzaldehyde complex **4o**$^+$$BF_4^-$ were recorded in CH_2Cl_2 utilizing a cell described earlier.[29] In all cases, π/σ ratios *increased* as temperatures *decreased*. Equilibrium constants were measured as above. Representative spectra are shown in Figure 3, and data are summarized in Table II, van't Hoff plots were linear,[30] as depicted in Figure 4, and gave the ΔH and ΔS values in Table II. These can be used to calculate ΔG and π/σ ratios for **4i,l,o**$^+$$BF_4^-$ in CH_2Cl_2 at other temperatures.

Next, ^{1}H NMR spectra of **4i,l,o**$^+$$BF_4^-$ were acquired over parallel temperature ranges in CD_2Cl_2. In each case, the chemical shift of the HC=O resonance varied markedly, moving upfield at lower temperatures. The chemical shift of the cyclopentadienyl resonance varied only moderately, moving downfield at lower temperatures. Data are summarized in Table III. Plots of mol fraction vs chemical shift gave limiting values of δ 5.85/6.06 for the HC=O and cyclopentadienyl resonances of π-**4o**$^+$$BF_4^-$ and δ 9.00/5.66 for those of σ-**4o**$^+$$BF_4^-$.[31]

Many ^{1}H, ^{13}C, and ^{31}P NMR spectra of **4**$^+$$BF_4^-$ were recorded between 0 and −96 °C in CD_2Cl_2—a limit imposed by the solvent freezing point. In nearly all cases, the chemical shifts of the HC=O and cyclopentadienyl ^{1}H and ^{13}C NMR resonances, and the PPh_3 ^{31}P NMR resonances, were temperature dependent. However, in no case did resonances of π and σ isomers decoalesce.

Table II. Temperature Dependence of the π/σ Equilibria of Aromatic Aldehyde Complexes **4i,l,o**$^+$$BF_4^-$ in CH_2Cl_2

complex	temp (K)	π/σ ratio	ΔH^a (kcal/mol)	ΔS^a (eu)
4i$^+$$BF_4^-$ [b]	303	73:27	3.6 ± 0.6	9.2 ± 2.0
	299	84:16		
	283	86:14		
	273	86:14		
	263	90:10		
	253	92:08		
	243	94:06		
	233	95:05		
4l$^+$$BF_4^-$	299	54:46	2.8 ± 0.2	9.1 ± 0.6
	283	61:39		
	273	65:35		
	263	69:31		
	253	72:28		
	243	79:21		
4o$^+$$BF_4^-$	299	15:85	1.8 ± 0.2	9.5 ± 0.6
	273	19:81		
	263	21:79		
	253	24:76		
	243	26:74		
	233	29:71		

[a] For $\pi \rightarrow \sigma$. [b] Optically active (+)-(*RS*)-**4i**$^+$$BF_4^-$ was used due to the low solubility of the racemate.

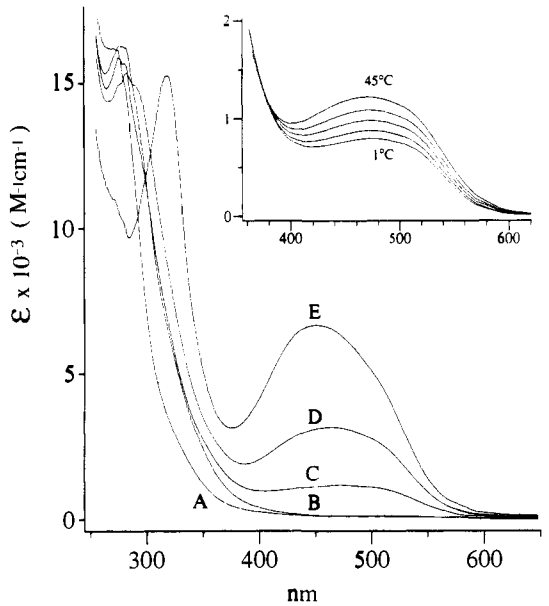

Figure 5. UV–visible spectra of aromatic aldehyde complexes (CH_2Cl_2, ambient temperature, 1.0–2.0 × 10^{-4} M): trace A, pentafluorobenzaldehyde complex **4a**$^+$$BF_4^-$; trace B, *p*-trifluoromethylbenzaldehyde complex **4b**$^+$$BF_4^-$; trace C, benzaldehyde complex **4i**$^+$$BF_4^-$; trace D, *p*-methylbenzaldehyde complex **4l**$^+$$BF_4^-$; trace E, *p*-methoxybenzaldehyde complex **4o**$^+$$BF_4^-$; inset, **4i**$^+$$BF_4^-$ at 45 (top), 30, 20, 10, and 1 °C.

Thus, the IR ν_{NO} absorptions of **4**$^+$$BF_4^-$ provide a unique means of quantifying π/σ equilibria. Significantly, as described elsewhere,[23,32] π and σ isomers of **4o**$^+$$BF_4^-$ do decoalesce when ^{31}P NMR spectra are recorded in a lower freezing solvent.

The solvent dependence of the π/σ equilibrium was also studied. The optically active benzaldehyde complex (+)-(*RS*)-**4i**$^+$$BF_4^-$ was dissolved in 75:25, 60:40, and 50:50 (v/v) CH_2Cl_2/hexane at 26 °C. This compound is much more soluble than the racemate in CH_2Cl_2/hexane mixtures. IR analyses indicated π/σ ratios of 81:19, 62:38, and 50:50—*lower* than that in pure CH_2Cl_2 (82:18; Scheme I). Similarly, the *p*-methoxybenzaldehyde complex **4o**$^+$$BF_4^-$ was dissolved in the more polar solvent CH_3NO_2. The π/σ ratio, 36:64, was *higher* than that in CH_2Cl_2 (15:85). Thus,

(29) Brinkman, K. C.; Blakeney, A. J.; Krone-Schmidt, W.; Gladysz, J. A. *Organometallics* **1984**, *3*, 1325.

(30) Benson, S. W. *Thermochemical Kinetics*, 2nd ed.; Wiley: New York, 1976; p 7.

(31) (a) The HC=O ^{1}H NMR chemical shift calculated for σ-**4o**$^+$$BF_4^-$ (δ 9.00) is similar to those of the iron-σ-isobutyraldehyde complex (η^5-C_5H_5)Fe(CO)$_2$(η^1-O=CHCH(CH$_3$)$_2$) (δ 9.58, CD_2Cl_2) and the adduct of BF_3 and *p*-methoxybenzaldehyde (δ 9.30, CH_2Cl_2).[31b,c] (b) Foxman, B. M.; Klemarczyk, P. T.; Liptrot, R. E.; Rosenblum, M. *J. Organomet. Chem.* **1980**, *187*, 253. (c) Grinvald, A.; Rabinovitz, M. *J. Chem. Soc., Perkin Trans. 2* **1974**, 94.

(32) (a) Quirós Méndez, N.; Mayne, C. L.; Gladysz, J. A. *Angew. Chem., Int. Ed. Engl.* **1990**, *29*, 1475. (b) Klein, D. P.; Quirós Méndez, N.; Boone, B. J.; Seyler, J. W.; Arif, A. M.; Gladysz, J. A., manuscripts in preparation.

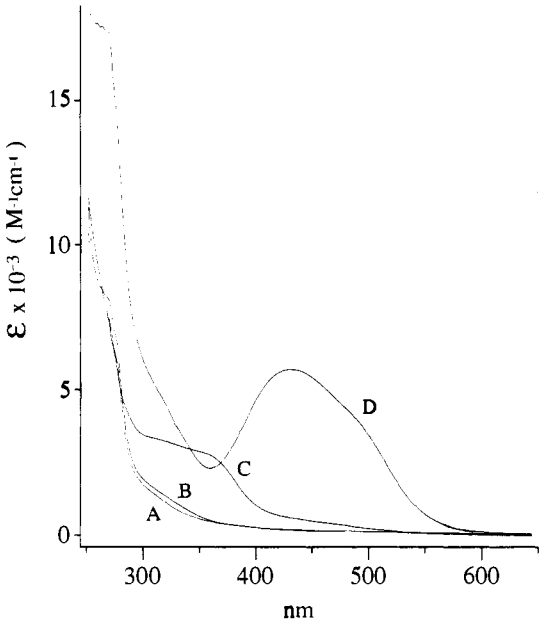

Figure 6. UV–visible spectra of ketone and aliphatic aldehyde complexes (CH_2Cl_2, ambient temperature, 1.0–1.7 × 10^{-4} M): trace A, formaldehyde complex $[(\eta^5\text{-}C_5H_5)Re(NO)(PPh_3)(\eta^2\text{-}O{=}CH_2)]^+BF_4^-$ (**3a**$^+BF_4^-$); trace B, acetaldehyde complex $[(\eta^5\text{-}C_5H_5)Re(NO)(PPh_3)(\eta^2\text{-}O{=}CHCH_3)]^+BF_4^-$ (**3b**$^+BF_4^-$); trace C, acetone complex $[(\eta^5\text{-}C_5H_5)Re(NO)(PPh_3)(\eta^1\text{-}O{=}C(CH_3)_2)]^+BF_4^-$ (**2a**$^+BF_4^-$); trace D, acetophenone complex $[(\eta^5\text{-}C_5H_5)Re(NO)(PPh_3)(\eta^1\text{-}O{=}C(CH_3)C_6H_5)]^+BF_4^-$ (**2b**$^+BF_4^-$).

less polar solvents decrease π/σ ratios, whereas more polar solvents increase π/σ ratios.[33]

4. UV–Visible Spectra. In the course of characterizing **4**$^+BF_4^-$, thermochromism was noted. For example, CH_2Cl_2 solutions of benzaldehyde complex **4i**$^+BF_4^-$ were orange at room temperature, but yellow below −40 °C. Similarly, CH_2Cl_2 solutions of *p*-methoxybenzaldehyde complex **4o**$^+BF_4^-$ were deep red at room temperature, but orange at −80 °C. In view of the increased equilibrium concentrations of σ isomers at high temperatures (Table II), this suggested that unique visible absorptions were associated with σ isomers.

Thus, UV–visible spectra of five representative complexes (**4a,b,i,l,o**$^+BF_4^-$) were recorded at ambient temperature, as shown in Figure 5. Variable temperature spectra of **4i**$^+BF_4^-$ were also obtained (inset). For comparison, UV–visible spectra of the π formaldehyde complex **3a**$^+BF_4^-$, π acetaldehyde complex **3b**$^+BF_4^-$, σ acetone complex **2a**$^+BF_4^-$ and σ acetophenone complex **2b**$^+BF_4^-$ are depicted in Figure 6. Note that all of these compounds contain PPh_3 phenyl rings that should give independent UV absorptions.

The 400–600-nm region of Figure 5 was analyzed first. The pentafluorobenzaldehyde complex **4a**$^+BF_4^-$ exhibited no well-defined absorptions, even at higher concentrations. An upper intensity limit of $\epsilon = 29$ M^{-1} cm^{-1} was assigned to a possible peak at 526 nm. The other complexes gave broad absorptions with maxima at 522, 472, 466, and 450 nm (ϵ 88, 1000, 3100, 6300 M^{-1} cm^{-1}). These diminished at lower temperatures (inset) and intensified as the equilibrium proportions of σ isomers of **4**$^+BF_4^-$ increased (Scheme I). Thus, they were assigned to the σ isomers. The shift to lower frequencies with electron-withdrawing substituents further suggests that they arise from metal-to-ligand charge transfer (MLCT).[34] Adducts of aromatic aldehydes and boron Lewis acids also exhibit visible absorptions,[35] but free aromatic aldehydes do not.

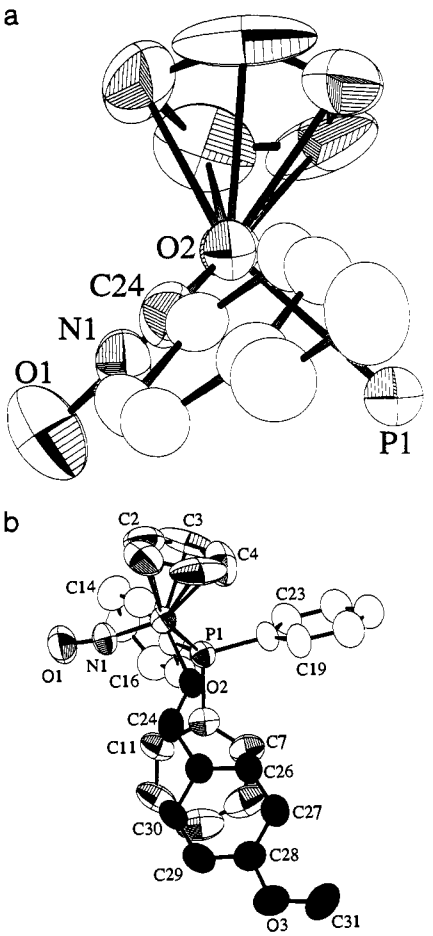

Figure 7. Views of the cation of *p*-methoxybenzaldehyde complex $[(\eta^5\text{-}C_5H_5)Re(NO)(PPh_3)(O{=}CH\text{-}4\text{-}C_6H_4OCH_3)]^+PF_6^-\cdot(CH_2Cl_2)_{0.5}$ (**4o**$^+PF_6^-\cdot(CH_2Cl_2)_{0.5}$): (a) Newman-type projection down the oxygen–rhenium bond with PPh_3 phenyl rings omitted, (b) relationship between the *p*-methoxybenzaldehyde ligand (darkened atoms) and C6–C11 PPh_3 phenyl ring (beneath, in approximate plane of paper), and partial numbering diagram (P–C_{ipso} = C6, C12, C18).

Some features in the 250–375-nm region of Figure 5 were absent in the spectra of the aliphatic aldehyde complexes in Figure 6. For example, **4a,b,i,l**$^+BF_4^-$ exhibited an increasingly red-shifted band (266–278 nm, ϵ 16 000–15 500 M^{-1} cm^{-1}). These likely have analogy in UV absorptions of uncomplexed benzaldehydes and arenes[36] and may originate from both σ and π binding modes. Also, **4o**$^+BF_4^-$ gave a unique intense absorption at 314 nm (ϵ 14 500 M^{-1} cm^{-1}). However, the UV spectrum of free *p*-methoxybenzaldehyde is very similar to that of *p*-methylbenzaldehyde (except for expected red shifts). We therefore speculate that the 314-nm band is due to charge transfer from a methoxy lone pair of σ-**4o**$^+BF_4^-$ to a vacant π^* orbital associated with the conjugated rhenium–aldehyde π system. This possibility is supported by a crystal structure described below.

The UV–visible spectrum of σ acetone complex **2a**$^+BF_4^-$ exhibited shoulders (312, 370 nm; ϵ 3200, 2400 M^{-1} cm^{-1}) that were absent in the spectra of π formaldehyde and acetaldehyde complexes **3a,b**$^+BF_4^-$ (Figure 6). These were presumed to be characteristic of the σ binding mode for aliphatic ketones. The σ acetophenone complex **2b**$^+BF_4^-$ gave a broad visible absorption analogous to those in Figure 5 but with a slight shoulder (434, 506 nm; ϵ 5200, 3000 M^{-1} cm^{-1}).

5. Solid-State Characterization. To date, only π aldehyde complexes of I have been structurally characterized.[15,16] Thus,

(33) Most solvents that are more polar than CH_2Cl_2 rapidly react with aldehyde complexes **4**$^+BF_4^-$ (e.g., CH_3CN, DMSO, alcohols) and are not suitable for π/σ ratio measurements.

(34) (a) Geoffroy, G. L.; Wrighton, M. S. *Organometallic Photochemistry*; Academic Press: New York, 1979; p 10. (b) If the ϵ value of the 522 nm absorption of σ-**4b**$^+BF_4^-$ is arbitrarily assumed to be 5200 M^{-1} cm^{-1} (that of **2b**$^+BF_4^-$), and the contribution of the UV tail to the experimentally measured absorption subtracted (corrected ϵ = 41 M^{-1} cm^{-1}), an equilibrium concentration of ca. 0.8% can be calculated for σ-**4b**$^+BF_4^-$. An analogous treatment of the possible 526-nm absorption of σ-**4a**$^+BF_4^-$ places an upper limit of 0.25% upon the equilibrium concentration.

(35) Rabinovitz, M.; Grinvale, A. *J. Am. Chem. Soc.* **1972**, *94*, 2724.

(36) *UV Atlas of Organic Compounds*; Plenum Press: New York, 1966.

Table III. Temperature Dependence of the HC=O and Cyclopentadienyl ^{1}H NMR Chemical Shifts of Aromatic Aldehyde Complexes **4i,l,o**$^+BF_4^-$

complex	temp (K)	% π isomer[a]	HC=O (δ)[b]	C_5H_5 (δ)[b]
4i$^+BF_4^-$[c]	303	73	6.79	5.89
	299	84	6.77	5.89
	283	86	6.70	5.90
	273	86	6.66	5.91
	263	90	6.62	5.92
	253	92	6.58	5.93
	243	94	6.55	5.94
	233	95	6.52	5.98
4l$^+BF_4^-$	299	54	7.33	5.82
	283	61	7.20	5.83
	273	65	7.11	5.84
	263	69	7.01	5.85
	253	72	6.94	5.86
	243	79	6.86	5.87
4o$^+BF_4^-$	299	15	8.54	5.72
	273	19	8.39	5.74
	263	21	8.32	5.75
	253	24	8.25	5.76
	243	26	8.18	5.77
	233	29	8.09	5.78

[a] Calculated from the VT-IR data in Table II. [b] In CD_2Cl_2 and referenced to internal $Si(CH_3)_4$. [c] Optically active (+)-(*RS*)-**4l**$^+BF_4^-$ was used due to the low solubility of the racemate.

Table IV. Summary of Crystallographic Data for *p*-Methoxybenzaldehyde Complex $[(\eta^5\text{-}C_5H_5)Re(NO)(PPh_3)(O{=}CH\text{-}4\text{-}C_6H_4OCH_3)]^+PF_6^-\cdot(CH_2Cl_2)_{0.5}$ (**4o**$^+PF_6^-\cdot(CH_2Cl_2)_{0.5}$)

molecular formula	$C_{31}H_{28}F_6NO_3P_2Re\cdot(CH_2Cl_2)_{0.5}$
molecular weight	867.2
crystal system	triclinic
space group	$P\bar{1}$
temp of collection	16 °C
cell dimensions	
a, Å	11.780(2)
b, Å	14.691(3)
c, Å	11.035(2)
α, deg	101.84(1)
β, deg	111.38(1)
γ, deg	82.32(1)
V, Å^3	1737(1)
Z	2
d_{calcd}, g/cm^3	1.66
d_{obs}, g/cm^3 (24 °C)	1.69 (CCl_4/CH_2I_2)
crystal dimensions, mm	0.33 × 0.25 × 0.10
radiation, Å	λ (Mo Kα) 0.71073
data collection method	θ–2θ
scan speed, deg/min	3
2θ scan range	$2 \le 2\theta \le 47$
reflcns measd	5257
scan range	$K\alpha_1 - 1.3$ to $K\alpha_2 + 1.6$
no. of reflcns between std	97
total unique data	5151
observed data, $I > 3\sigma(I)$	3958
abs. coeff. (μ), cm^{-1}	37.8
no. of variables	425
$R = \sum\|\|F_o\| - \|F_c\|\|/\sum\|F_o\|$	0.0491
$R_w = \sum\|\|F_o\| - \|F_c\|\|w^{1/2}/\sum\|F_o\|w^{1/2}$	0.0599
goodness of fit	2.99
weighting factor, *w*	unit weight
Δρ (max), e/Å^3	1.652 e/Å^3, ca. 1.16 Å from Re

we sought crystals of a σ isomer of **4**$^+X^-$. The methoxy-substituted complexes **4m,n,o**$^+X^-$, which are predominantly σ isomers in solution, gave deep burgundy crystals. X-ray data were acquired on **4o**$^+PF_6^-\cdot(CH_2Cl_2)_{0.5}$ as summarized in Table IV. Refinement afforded the structures shown in Figure 7. Key bond lengths, bond angles, and torsion angles are summarized in Table V. The HC=O hydrogen was not located. However, a position was calculated based upon an idealized sp^2 carbon geometry.

Features of the *p*-methoxybenzaldehyde ligand were analyzed. The N–Re–O2–C24 and P–Re–O2–C24 torsion angles were −0.5° and −91.0°, respectively. These closely match the 0° and ±90° angles of the idealized Re–O rotamer II (Chart I). The least squares plane of the aryl carbons (C25–C30) was calculated. This plane made a 6.0° angle with the C=O bond and a 5.6° angle with the HC=O plane. The O2–C24–C25–C26 torsion angle was also close to 0° (3°), and the companion O2–C24–C25–C30 torsion angle was −174°. These data indicate a very high degree of aryl/C=O conjugation. The methoxy group carbon–oxygen bond appeared to be coplanar with the arene ring. Accordingly, the C31–O3–C28–C27 and C31–O3–C28–C29 torsion angles were near 0° and ±180° (0°, −177°).

Table V. Selected Bond Lengths (Å), Bond Angles (deg), and Torsion Angles (deg) in **4o**$^+PF_6^-\cdot(CH_2Cl_2)_{0.5}$

Re–O2	2.080(5)	C3–C4	1.39(2)
O2–C24	1.271(8)	C4–C5	1.22(2)
Re–P1	2.397(2)	C5–C1	1.52(2)
Re–N	1.731(6)	C24–C25	1.44(1)
N–O1	1.208(7)	C25–C26	1.363(9)
Re–C1	2.275(9)	C26–C27	1.38(1)
Re–C2	2.20(1)	C27–C28	1.39(1)
Re–C3	2.22(1)	C28–C29	1.39(1)
Re–C4	2.24(1)	C28–O3	1.360(9)
Re–C5	2.295(9)	C29–C30	1.38(1)
C1–C2	1.39(2)	C30–C25	1.42(1)
C2–C3	1.29(2)	C31–O3	1.41(1)
N–Re–P1	92.0(2)	C27–C28–O3	123.5(8)
Re–N–O1	170.3(6)	C28–C29–C30	119.7(7)
N–Re–O2	102.9(2)	C28–O3–C31	119.0(7)
P1–Re–O2	83.3(1)	C29–C30–C25	119.6(7)
Re–O2–C24	129.5(4)	C29–C28–O3	115.1(7)
O2–C24–C25	122.2(6)	C30–C25–C26	118.6(7)
C24–C25–C26	124.6(7)	C1–C2–C3	110(1)
C25–C26–C27	123.2(7)	C2–C3–C4	110(1)
C26–C27–C28	117.5(7)	C3–C4–C5	109(1)
C27–C28–C29	121.3(7)	C4–C5–C1	110(1)
P–Re–O2–C24	−91.1(9)	O2–C24–C25–C26	3(2)
N–Re–O2–C24	−0.5(10)	O2–C24–C25–C30	−174(1)
C31–O3–C28–C27	0(2)	C31–O3–C28–C29	−177(2)
O2–Re–P1–C6	30.9(5)		

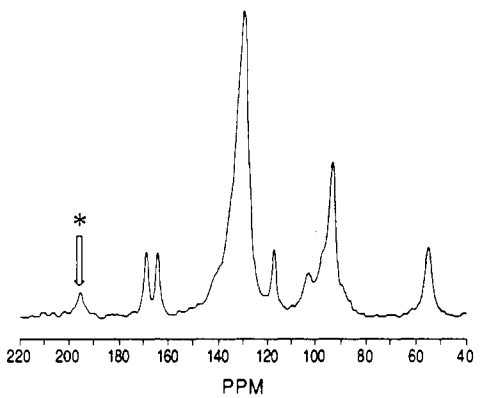

Figure 8. CPMAS ^{13}C NMR spectrum of a CH_2Cl_2 hemisolvate of 2,4-dimethoxybenzaldehyde complex $[(\eta^5\text{-}C_5H_5)Re(NO)(PPh_3)(O{=}CH\text{-}2,4\text{-}C_6H_4(OCH_3)_2)]^+BF_4^-$ (**4m**$^+BF_4^-\cdot(CH_2Cl_2)_{0.5}$). The * indicates the H*C*=O resonance (196.2 ppm).

As a further check on solid-state structure, the CPMAS ^{13}C NMR spectrum of 2,4-dimethoxybenzaldehyde complex **4m**$^+BF_4^-$ was recorded (Figure 8). The HC=O resonance (196.2 ppm) shifted 29 ppm downfield from that in CD_2Cl_2 (167.3 ppm, Table I), consistent with a large increase in the proportion of σ isomer. However, other resonances were within 1 ppm of those found in CD_2Cl_2.[37] The CPMAS ^{13}C NMR spectra of the predominantly

(37) CPMAS ^{13}C NMR spectral data (ppm, referenced to external $C_6(CH_3)_6$): **4a**$^+BF_4^-$, 132.5 (br s, PPh_3/Ar), 102.2 (br s, C_5H_5); **4l**$^+BF_4^-$, 130.9 (br s, PPh_3/Ar), 101.2 (br s, C_5H_5); **4m**$^+BF_4^-$, 196.2 (s, HCO), 169.6 (s, *C*-OCH_3), 165.4 (s, *C*-OCH_3), 132.3 (br s, PPh_3), 119.2 (s, *C*-CHO), 105.4 (sh, Ar), 99.2 (sh, Ar), 96.2 (br s, C_5H_5), 56.9 (s, OCH_3). Complexes **4a,l**$^+BF_4^-$ are not as crystalline as **4m**$^+BF_4^-$. This is presumed to adversely affect the tumbling characteristics of the solid samples.

π complexes **4a,i**$^+BF_4^-$ were also recorded. Unfortunately, broader resonances and poorer signal/noise ratios were obtained. Thus, only cyclopentadienyl and aryl carbon resonances were observed.[37] However, the chemical shift trends of the former paralleled those in CD_2Cl_2.

Discussion

1. Effect of Ligand upon π/σ Equilibria. The π/σ equilibrium data for aromatic aldehyde complexes **4**$^+BF_4^-$ (Scheme I, Table II) illustrate a variety of trends. To begin, contrast the π/σ ratio for benzaldehyde complex **4i**$^+BF_4^-$ (84:16) to those of aliphatic aldehyde complexes **3**$^+X^-$. For the latter, IR data indicate >96:<4 π/σ mixtures, even with the bulky ligand pivalaldehyde.[15] Thus, a phenyl C=O substituent stabilizes the σ binding mode relative to aliphatic substituents.

We suggest that this is mainly a reasonance effect. In a σ isomer, an aryl group can conjugate with the C=O—Re π assembly, providing a modest stability enhancement. Such interactions are evidenced in the crystal structure of **4o**$^+PF_6^-$ (Figure 7), and UV–visible spectra (Figure 5). In contrast, π isomers are best represented by the metallacyclic resonance form B (eq i), and aryl/C$\tau\tau$O resonance stabilization is diminished.

However, there is a possibility that σ isomers are also stabilized by π interactions between the aryl/C=O moieties and PPh_3 phenyl rings. Figure 7b shows that the C=O group of **4o**$^+PF_6^-$ (C24, O2) resides above the ipso and ortho carbons of a PPh_3 phenyl ring (C11, C6), with a O2–Re–P1–C6 torsion angle of 30.9°. The two phenyl rings are roughly parallel (angle of least squares planes = 12°), with plane/atom separations that range from 3.4 (C25) to 3.9 (C27) Å and 3.0 (C11) to 3.6 (C8) Å. The acetophenone complex **2b**$^+PF_6^-$ adopts a similar structure, with a 4° angle between the corresponding phenyl rings.[14a]

Strong electronic effects of aryl substituents upon π/σ equilibria are also evident in Scheme I. To a first approximation, electron withdrawing groups favor π binding, and donor groups favor σ binding. The former enhance aldehyde ligand π acidity and lower σ basicity, whereas the latter have an opposite effect. For reasons outlined above, backbonding into the aldehyde π acceptor orbital is much stronger in the π binding mode, while aldehyde σ basicity provides the dominant bonding interaction in the σ binding mode. These factors, which have also been analyzed in a recent theoretical study,[10] appear to be the primary determinants of π/σ equilibrium ratios within this family of complexes.

From this analysis, similar π/σ ratios might have been expected for the *o*- and *p*-methoxybenzaldehyde complexes **4e,o**$^+BF_4^-$. However, that of **4e**$^+BF_4^-$ is much higher and very close to that of *m*-methoxybenzaldehyde complex **4d**$^+BF_4^-$. In fact, the equilibrium and reactivity properties of *o*- and *p*-methoxy substituted Ar(C=O)X compounds often differ markedly.[38] Among the many rationales proposed, the dominant factor appears to be weaker resonance donation from the *o*-methoxy group, due at least in part to steric inhibition of Ar/C=O conjugation. In the case of **4e**$^+BF_4^-$, diminished Ar/C=O conjugation would attenuate the σ-stabilizing interactions noted above and enhance π-stabilizing interactions. The effects of *o*- and *m*-methoxy substituents are also similar in the *p*-methoxy derivatives **4m,n**$^+BF_4^-$.

The IR ν_{NO} of both π and σ isomers decreases roughly monotonically in the series **4a–o**$^+BF_4^-$ (π: 1745 → 1733 cm^{-1}; σ: 1701 → 1692 cm^{-1}), consistent with the effect of progressively more donating aryl substituents upon aldehyde π acceptor and σ donor properties.[22] A Hammett plot of log (K/K_0) versus σ^+ for the *p*- and *m*- monosubstituted benzaldehyde complexes that give IR-detectable amounts of both isomers (**4d,f,g,i,k,l,o**$^+BF_4^-$) is only roughly linear ($R^2 = 0.956$).[39] Nonetheless, ρ is clearly negative (−1.9). A three-point plot of ΔH versus σ^+ for **4i,l,o**$^+BF_4^-$ is linear ($R^2 = 0.999$).

Analogous electronic effects upon π/σ equilibria have been documented in ketone complexes **2**$^+X^-$.[17] For example, fluoroacetone and pentafluoroacetophenone complexes exist as mixtures of π and σ isomers (ν_{NO} 1745–1749 and 1699–1695 cm^{-1}). Only π isomers of 1,3-dichloroacetone and 1,3-difluoroacetone complexes are observed (ν_{NO} 1740–1762 cm^{-1}). Thus, within IR detection limits, ketones can bind in an entirely π *or* σ manner to the Lewis acid I. In contrast, aromatic aldehydes **6a–o** always give detectable quantities of π isomers.

2. Effect of Rhenium Fragment, Temperature, and Solvent upon π/σ Equilibria. The pentamethylcyclopentadienyl analog of benzaldehyde complex **4i**$^+BF_4^-$, $[(\eta^5\text{-}C_5Me_5)Re(NO)(PPh_3)(O{=}CHC_6H_5)]^+BF_4^-$, has recently been reported.[40] Pentamethylcyclopentadienyl ligands are more electron-releasing than cyclopentadienyl ligands.[13e,41] Thus, the enhanced π basicity and/or diminished σ acidity of the rhenium fragment might have been expected to give greater π/σ ratios. However, the greater bulk should have an opposite effect, for as noted above both C=O substituents can sterically interact with ligands on rhenium in the π binding mode. In actuality, the π/σ ratio (78:22; ν_{NO} 1719, 1684 cm^{-1}) is similar. Hence, the electronic and steric effects approximately cancel.

Table II illustrates the marked temperature dependence of the π/σ equilibria. One beneficial consequence is that ΔH and ΔS values are easily determined. The former show that $\pi \rightarrow \sigma$ isomerization is in all cases endothermic, even for the predominantly σ complex **4o**$^+BF_4^-$ (ΔH 1.8 kcal/mol). However, $\pi \rightarrow \sigma$ isomerization is favored entropically, with ΔS falling in a narrow positive range (9.1–9.5 eu). The σ isomers obviously possess more conformational degrees of freedom and as analyzed below are likely less strongly solvated.

The temperature dependence of the π/σ equilibria affects variable temperature NMR spectra. For example, the chemical shifts of the PPh_3 ^{31}P and HC=O ^1H and ^{13}C resonances, all of which differ greatly in the π and σ limits, can vary dramatically. Also, since most of the equilibria in Scheme I are biased toward π isomers, and the π/σ ratios increase further at lower temperatures, it is difficult to observe the decoalescence of π and σ isomers. To date, separate resonances for π and σ isomers have been found only in the case of **4o**$^+BF_4^-$ (^{31}P) at temperatures below 180 K in the freon solvent $CDFCl_2$.[32a] As expected, the π/σ ratio (72:28, 136 K) is much higher than that in Scheme I.

The π/σ equilibrium ratios also increase with increasing solvent polarity (CH_3NO_2 > CH_2Cl_2 > hexane). We provisionally attribute this to the relative magnitude of positive charge delocalization in π and σ isomers. As discussed above, the aryl/C=O—Re linkages are more highly conjugated in σ isomers. This allows extended charge delocalization, and solvation is diminished, consistent with the ΔS data. The charge in π isomers remains more localized, resulting in enhanced solvation energy and stability in polar solvents.

3. Related π/σ Equilibria. Other ligands that give similar π/σ equilibria include nitriles (RC≡N),[42] diazenes (RN=NR),[43] dinitrogen (N≡N),[44] dithioesters (RS(R)C=S),[45] phosphaalkenes ($R_2C{=}PR$),[46] and aromatic heterocycles such as pyridines,[47]

(38) (a) Wolfenden, R.; Jencks, W. P. *J. Am. Chem. Soc.* **1961**, *83*, 2763 and references therein. (b) See, also: Charton, M. *Prog. Phys. Org. Chem.* **1971**, *8*, 235.

(39) Exner, O. In *Correlation Analysis in Chemistry*; Chapman, N. B., Shorter, J., Eds.; Plenum: New York, 1978; Chapter 10.

(40) Agbossou, F.; Ramsden, J. A.; Huang, Y.-H.; Arif, A. M.; Gladysz, J. A. *Organometallics* **1992**, *11*, 693.

(41) (a) Choi, M.-G.; Robertson, M. J.; Angelici, R. J. *J. Am. Chem. Soc.* **1991**, *113*, 4005. (b) Choi, M.-G.; Angelici, R. J. *J. Am. Chem. Soc.* **1991**, *113*, 5651.

(42) (a) Birk, R.; Berke, H.; Hund, H.-U.; Huttner, G.; Zsolnai, L.; Dahlenburg, L.; Behrens, U.; Sielisch, T. *J. Organomet. Chem.* **1989**, *372*, 397. (b) see also Roth, T.; Kaim, W. *Inorg. Chem.* **1992**, *31*, 1930.

(43) (a) Einstein, F. W. B.; Sutton, D.; Tyers, K. G. *Inorg. Chem.* **1987**, *26*, 111. (b) Kang, S.-K.; Albright, T. A.; Mealli, C. *Inorg. Chem.* **1987**, *26*, 3158.

(44) Cusanelli, A.; Sutton, D. *J. Chem. Soc., Chem. Commun.* **1989**, 1719.

(45) Schenk, W. A.; Rüb, D.; Burschka, C. *J. Organomet. Chem.* **1987**, *328*, 287.

(46) (a) van der Knaap, T. A.; Bickelhaupt, F.; Kraaykamp, J. G.; van Koten, G.; Bernards, J. P. C.; Edzes, H. T.; Veeman, W. S.; de Boer, E.; Baerends, E. J. *Organometallics* **1984**, *3*, 1804. (b) Nixon, J. F. *Chem. Rev.* **1988**, *88*, 1327. (c) See also: Jutzi, P.; Meyer, U.; Opiela, S.; Neumann, B.; Stammler, H.-G. *J. Organomet. Chem.* **1992**, *439*, 279.

Scheme II. Other Relevant π/σ Equilibria

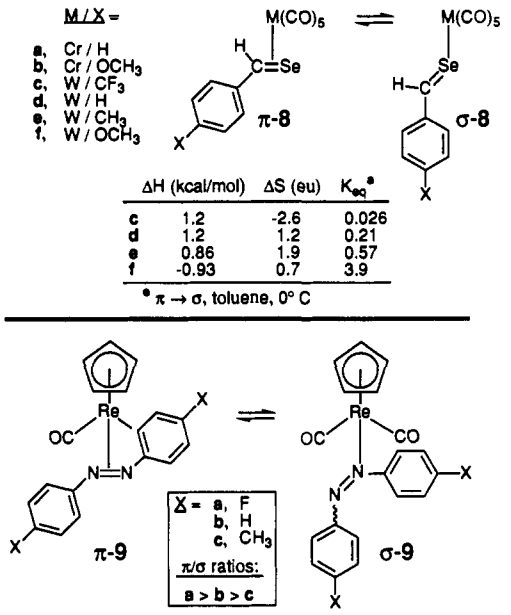

thiophenes, and selenophenes,[41] However, detailed studies by H. Fischer of neutral group IV thiobenzaldehyde and selenobenzaldehyde complexes, $(CO)_5M(S{=}CHAr)$ and $(CO)_5M(Se{=}CHAr)$ (**8**),[48] are of particular relevance to our data and will be considered first. Representative complexes are given in Scheme II.

The data for **8** in Scheme II show that aryl substituents exert an electronic effect upon π/σ equilibria very similar to that in Scheme I. A plot of log (K/K_o) versus σ^+ for **8c–f** is linear (R^2 = 0.999; toluene, 0 °C), with a ρ value (−1.65) close to that found for $\mathbf{4}^+BF_4^-$. Also, π/σ ratios increase with a decrease in temperature, and a *decrease* in solvent polarity. The former trend parallels that of $\mathbf{4}^+BF_4^-$, but the latter differs. Note that in contrast to $\mathbf{4}^+BF_4^-$, **8** carries no formal charge. Thus, the solvation energy will primarily be determined by dipole/dipole interactions, as opposed to stronger charge/dipole interactions possible with $\mathbf{4}^+BF_4^-$. Intuitively, it seems plausible that the C⇀Se bond dipole and molecular dipole should be greater in σ-**8** than π-**8**. Hence, σ-**8** should be more highly stabilized in polar solvents. Interestingly, **8a–f** are also thermochromic, with the σ isomers exhibiting visible MLCT absorptions.

Ligand-based electronic effects upon π/σ equilibria have also been reported by Sutton with rhenium diazene complexes of the type $(\eta^5\text{-}C_5H_5)Re(CO)_2(ArN{=}NAr)$ (**9**).[43a] As illustrated in Scheme II, π/σ ratios decrease in the order Ar = 4-C_6H_4F > C_6H_5 > 4-$C_6H_4CH_3$, paralleling the data for $\mathbf{4}^+BF_4^-$ and **8**. Complementary electronic effects involving metal fragments have also been found. For example, π/σ ratios of **8** decrease in the order M = W > Cr.[48] This follows the π basicity order of the corresponding $M(CO)_5$ moieties. Similarly, Angelici finds that for rhenium–selenophene complexes of the formula $(\eta^5\text{-}C_5R_5)Re(CO)_2(SeC_4H_4)$, the π/σ ratio when R = H, 25:75, reverses to >98:<2 when R = CH_3 ($CDCl_3$, ambient temperature).[41b] Comparable metal and ligand-based electronic effects have also been observed in π/σ equilibria of phosphaalkene complexes.[46]

Finally, many aldehyde and ketone complexes of the pentaammineosmium and ruthenium fragments have been prepared by Harman, Taube, and Lay.[9] They have carefully studied the effect of the metal oxidation state upon π/σ equilibria utilizing electrochemical techniques. For the osmium(II) and ruthenium(II)

Scheme III. Other Structurally Characterized Transition Metal σ Complexes of Unsaturated Aldehydes

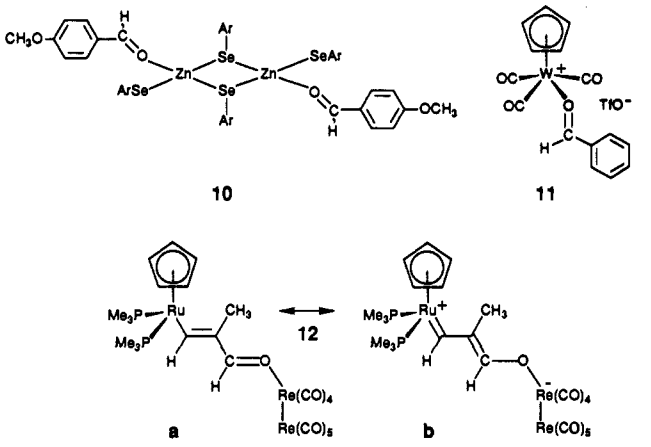

acetone complexes $[(H_3N)_5M(O{=}C(CH_3)_2)]^{2+}$, $\Delta G°$ for $\pi \rightarrow \sigma$ isomerism are 5.0 and 1.7 kcal/mol (acetone, 25 °C), respectively. However, for the osmium(III) and ruthenium(III) complexes $[(H_3N)_5M(O{=}C(CH_3)_2)]^{3+}$, the corresponding $\Delta G°$ are ca. −16 and −1.6 kcal/mol. Thus, π/σ ratios are much higher for the more reduced or π basic metal fragments.

4. Other Structural and Equilibrium Properties. Additional structural features of $\mathbf{4}^+X^-$ merit analysis. For example, σ isomers can in theory exhibit C=O geometric isomerism. Based upon steric considerations, the trans (*E*) isomers depicted in Scheme I would be expected to greatly dominate. Accordingly, $\mathbf{4o}^+PF_6^-$ crystallizes as a trans isomer (Figure 7). However, NMR experiments with acetone complex $\mathbf{2a}^+BF_4^-$ and higher homologs show that cis/trans C=O substituents undergo rapid intramolecular exchange, with $\Delta G^{\ddagger}_{133\text{–}151K}$ of only 6–7 kcal/mol.[14] Thus, small equilibrium concentrations of cis isomers of σ-$\mathbf{4}^+X^-$ are likely kinetically accessible in solution.

The C=O bond of $\mathbf{4o}^+PF_6^-$ (1.271 (8) Å) appears to be slightly longer than those in σ-acetone and acetophenone complexes $\mathbf{2a,b}^+PF_6^-$ (1.248(9), 1.245(8) Å)[14a] and the dimeric zinc *p*-methoxybenzaldehyde complex $[Zn(Se\text{-}2,4,6\text{-}C_6H_2(t\text{-}C_4H_9)_3)_2(\eta^1\text{-}O{=}CH\text{-}4\text{-}C_6H_4OCH_3)]_2$ (**10**; 1.242(10) Å) shown in Scheme III.[8g] The C=O bond is distinctly longer than those in the tungsten–σ-benzaldehyde complex $[(\eta^5\text{-}C_5H_5)W(CO)_3(\eta^1\text{-}O{=}CHC_6H_5)]^+TfO^-$ (**11**, 1.21(1) Å)[49] and the manganese–σ-aldehyde complex $Mn_2(CO)_9(\eta^1\text{-}O{=}CHCH_2R)$ (1.216(9) Å),[50] To our knowledge, the C=O bond length in free *p*-methoxybenzaldehyde is unknown. However, that in *p,p'*-dimethoxybenzophenone is 1.211–1.213 Å.[51]

Two electronic factors may contribute to the C=O bond lengthening in $\mathbf{4o}^+PF_6^-$, as illustrated by the generalized resonance forms in eq ii. First, the stronger the Lewis acidity of the metal

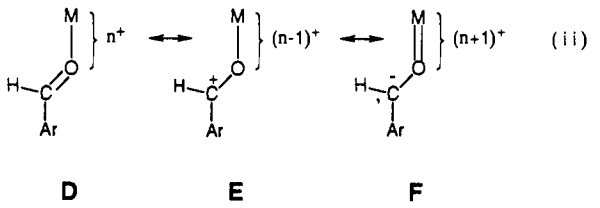

fragment (and donor properties of the aryl group), the greater the contribution by resonance form **E**. Second, the stronger the π basicity of the metal fragment (and acceptor properties of the aryl group), the greater the contribution by resonance form **F**. In each case, the carbon–oxygen bond order is one. The rhenium fragment I is not significantly more Lewis acidic than other metal

(47) (a) Covert, K. J.; Neithamer, D. R.; Zonnevylle, M. C.; LaPointe, R. E.; Schaller, C. P.; Wolczanski, P. T. *Inorg. Chem.* **1991**, *30*, 2494. (b) See, also: Gray, S. D.; Smith, D. P.; Bruck, M. A.; Wigley, D. E. *J. Am. Chem. Soc.* **1992**, *114*, 5462.

(48) (a) Fischer, H.; Zeuner, S.; Gerbing, U.; Riede, J.; Kreiter, C. G. *J. Organomet. Chem.* **1989**, *377*, 105. (b) Fischer, H.; Zeuner, S. *Z. Naturforsch., B: Anorg. Chem., Org. Chem.* **1985**, *40b*, 954.

(49) Song, J.-S.; Bullock, R. M.; Szalda, D. J., Brookhaven National Laboratory, personal communication of manuscript in preparation.

(50) Bullock, R. M.; Rappoli, B. J.; Samsel, E. G.; Rheingold, A. L. *J. Chem. Soc., Chem. Commun.* **1989**, 261.

(51) Norment, H. G.; Karle, I. L. *Acta. Crystallogr.* **1962**, *15*, 873.

fragments, but it is a distinctly superior π donor.[13] Consequently, we propose that both **E** and **F** are to comparable extents responsible for the longer C=O bond. A similar C=O bond length is found in the β-metalated rhenium–α-methylacrolein complex **12** (Scheme III; 1.263(12) Å).[52] In this case, the strong donor properties of the β substituent likely result in a substantial contribution by resonance form **12b** (≡**E**).

Complex **4o**$^+$$PF_6^-$ exhibits smaller N–Re–O–C torsion and Re–O–C bond angles (0°; 129.5(4)°) than acetone and acetophenone complexes **2a,b**$^+$$PF_6^-$ (21°, 9°; 136.3(4)°, 138.3(4)°).[14a] This likely reflects the larger size of the cis C=O substituents in **2a,b**$^+$$PF_6^-$ (methyl), which are directed toward the nitrosyl ligand. Previously, the crystal structures of methoxy arenes have been carefully analyzed by Kollman and Houk.[53] The arene rings and O–CH_3 bonds are nearly always coplanar, as in **4o**$^+$$PF_6^-$. Further, of the two C–C–O–CH_3 bond angles, that in which the methoxy group is syn to an aryl hydrogen averages 6° greater. Accordingly, the C27–C28–O3 bond angle in **4o**$^+$$PF_6^-$ (123.5(8)°) is 8.3° larger than the C29–C28–O3 bond angle (115.1(7)°).

Finally, π isomers of **4**$^+$$BF_4^-$ can exist as two configurational diastereomers that differ in the aldehyde enantioface bound to rhenium. The isomer shown in Chart I (III) greatly dominates. However, as communicated earlier,[32a] small equilibrium concentrations of the other can be detected by low-temperature NMR. Thus, the equilibrium data in Scheme I are for the aggregate population of both π isomers. These diastereomeric equilibria do not show a detectable temperature dependence, and full details will be reported separately.[32b]

5. Summary and Prospective. We have shown that π/σ equilibria in metal complexes of organic carbonyl compounds can be a sensitive function of the electronic properties of the ligand, the solvent, and the temperature. Others have demonstrated that the electronic properties of the metal fragment can also be of considerable importance.[9] Trends in our equilibrium data are paralleled with other classes of ligands.[41,44,46,48] Thus, some of the generalizations given above for aromatic aldehyde complexes **4**$^+$$X^-$ may have broad applicability.

This paper also lays the necessary foundation for subsequent research on several important subjects. For example, **4**$^+$$X^-$ are attractive substrates for studies of *rates* of interconversion of π and σ isomers, and structural trends within each series of isomers. Also, ketone complexes **2**$^+$$X^-$, aliphatic aldehyde complexes **3**$^+$$X^-$, and **4**$^+$$X^-$ all undergo highly diastereoselective reactions with nucleophiles.[14a,15a,54,55] Rate experiments with **4**$^+$$X^-$ may allow the relative reactivities of σ and π isomers toward nucleophiles, and the attendant mechanisms of diastereoselection, to be determined. Future reports will describe progress toward these objectives.[55]

Experimental Section

General Methods. General procedures have been described in a recent paper.[14] VT NMR spectra were recorded on Varian XL-300 spectrometers as previously detailed.[56] Samples were thoroughly degassed (freeze–pump–thaw × 3), and probe temperatures were calibrated with methanol. UV–visible spectra were recorded on an HP-8452A spectrometer. CPMAS ^{13}C NMR spectra were acquired on a Bruker 200 MHz spectrometer.

Solvents were purified as follows: hexane, distilled from Na/benzopenone; benzene, filtered through activated alumina and distilled from Na/benzophenone; ether, distilled from $LiAlH_4$ and then Na/benzophenone; CH_2Cl_2, distilled from P_2O_5 or CaH_2; CD_2Cl_2, vacuum transferred from CaH_2. HBF_4·OEt_2 was standardized as described earlier.[12] Aldehydes were obtained from common commercial sources and used without purification. The labeled aldehyde $C_6H_5(^{13}C{=}O)H$ (98 atom%) was used as received from MSD Isotopes, and 4-$CH_3OC_6H_4(C{=}O)D$ was prepared from methyl *p*-methoxybenzoate (Aldrich) by standard $LiAlD_4$ reduction/PCC oxidation procedures.[57] The corresponding complexes were synthesized by procedures analogous to those given below.

[(η^5-C_5H_5)Re(NO)(PPh$_3$)(O=CHC$_6$F$_5$)]$^+$$BF_4^-$ (4a$^+$$BF_4^-$). A Schlenk flask was charged with (η^5-C_5H_5)Re(NO)(PPh$_3$)(CH_3) (**5**,[18] 0.301 g, 0.539 mmol), CH_2Cl_2 (15 mL), and a stir bar and was cooled to −80 °C. Then HBF_4·OEt_2 (0.081 mL, 0.60 mmol) and pentafluorobenzaldehyde (0.165 mL, 1.3 mmol) were added with stirring. After 0.5 h, the cooling bath was removed. After an additional 1 h, ether (30 mL) was added. The resulting light yellow precipitate was collected by filtration, washed with ether (3 × 10 mL), and dried under oil pump vacuum to give **4a**$^+$$BF_4^-$ (0.420 g, 0.508 mmol, 94%). A sample was dissolved in CH_2Cl_2. Ether was slowly added by vapor diffusion. Light yellow needles formed, which were collected by filtration, washed with ether (3 × 2 mL), and dried under oil pump vacuum: mp 146–148 °C dec. Anal.[58]

[(η^5-C_5H_5)Re(NO)(PPh$_3$)(O=CH-4-$C_6H_4CF_3$)]$^+$$X^-$ (4b$^+$$X^-$). A. Complex **5** (0.312 g, 0.559 mmol), CH_2Cl_2 (5 mL), HBF_4·OEt_2 (0.084 mL, 0.62 mmol), and *p*-trifluoromethylbenzaldehyde (0.229 mL, 1.68 mmol) were combined in a procedure analogous to that given for **4a**$^+$$BF_4^-$. An identical workup gave **4b**$^+$$BF_4^-$ (0.362 g, 0.450 mmol, 80%) as a bright yellow powder. A sample was dissolved in 4:3 CH_2Cl_2/ether (v/v), and a layer of ether was added. Small bronze needles of **4b**$^+$$BF_4^-$ formed: mp 188–191 °C dec. Anal.[58] **B.** A Schlenk flask was charged with (η^5-C_5H_5)Re(NO)(PPh$_3$)(H) (**7**,[21] 0.142 g, 0.260 mmol), CH_2Cl_2 (4 mL), and a stir bar and was cooled to −80 °C. Then $Ph_3C^+PF_6^-$ (0.101 g, 0.259 mmol) and *p*-trifluoromethylbenzaldehyde (0.178 mL, 1.30 mmol) were added with stirring. The cooling bath was removed. After 2 h, ether was added. A dark tan powder formed, which was collected by filtration, washed with ether (3 × 10 mL), and dried under oil pump vacuum to give **4b**$^+$$PF_6^-$ (0.171 g, 0.199 mmol, 76%). A sample was dissolved in CH_2Cl_2 and layered with ether at −24 °C. Bronze prisms of **4b**$^+$$PF_6^-$ formed: mp 183–187 °C dec. Anal.[58] Alternatively, recrystallization from CH_2Cl_2/pentane (25 °C) also gave bronze prisms of **4b**$^+$$PF_6^-$: mp 187–192 °C dec. Anal.[58]

[(η^5-C_5H_5)Re(NO)(PPh$_3$)(O=CH-3-$C_6H_4CF_3$)]$^+$$BF_4^-$ (4c$^+$$BF_4^-$). Complex **5** (0.232 g, 0.416 mmol), CH_2Cl_2 (3 mL), HBF_4·OEt_2 (0.062 mL, 0.46 mmol), and *m*-trifluoromethylbenzaldehyde (0.167 mL, 1.25 mmol) were combined in a procedure analogous to that given for **4a**$^+$$BF_4^-$. An identical workup gave **4c**$^+$$BF_4^-$ (0.317 g, 0.394 mmol, 95%) as a bright yellow powder. A sample was dissolved in CH_2Cl_2 and layered with ether. Small bronze cubes of **4c**$^+$$BF_4^-$ formed: mp 180–183 °C dec. Anal.[58]

[(η^5-C_5H_5)Re(NO)(PPh$_3$)(O=CH-3-$C_6H_4OCH_3$)]$^+$$BF_4^-$ (4d$^+$$BF_4^-$). Complex **5** (0.209 g, 0.374 mmol), CH_2Cl_2 (3 mL), HBF_4·OEt_2 (0.056 mL, 0.41 mmol), and *m*-methoxybenzaldehyde (0.136 mL, 1.12 mmol) were combined in a procedure analogous to that given for **4a**$^+$$BF_4^-$. An identical workup gave **4d**$^+$$BF_4^-$ (0.279 g, 0.364 mmol, 97%) as a bright yellow powder. A sample was dissolved in 3:1 CH_2Cl_2/ether (v/v) and ether was added by vapor diffusion. Bronze microcrystals of **4d**$^+$$BF_4^-$ formed: mp 146–148 °C dec. Anal.[58]

[(η^5-C_5H_5)Re(NO)(PPh$_3$)(O=CH-2-$C_6H_4OCH_3$)]$^+$$BF_4^-$ (4e$^+$$BF_4^-$). Complex **5** (0.203 g, 0.363 mmol), CH_2Cl_2 (5 mL), HBF_4·OEt_2 (0.054 mL, 0.40 mmol), and *o*-methoxybenzaldehyde (0.123 mL, 1.09 mmol) were combined in a procedure analogous to that given for **4a**$^+$$BF_4^-$. An identical workup gave **4e**$^+$$BF_4^-$ (0.253 g, 0.330 mmol, 91%) as a bright yellow powder. A sample was dissolved in 4:1 CH_2Cl_2/ether (v/v) and layered with ether. Small bronze prisms of **4e**$^+$$BF_4^-$ formed: mp 191–193 °C dec. Anal.[58]

[(η^5-C_5H_5)Re(NO)(PPh$_3$)(O=CH-4-C_6H_4Cl)]$^+$$BF_4^-$ (4f$^+$$BF_4^-$). Complex **5** (0.205 g, 0.368 mmol), CH_2Cl_2 (3 mL), HBF_4·OEt_2 (0.055 mL, 0.40 mmol), and *p*-chlorobenzaldehyde (0.155 g, 1.10 mmol) were combined in a procedure analogous to that given for **4a**$^+$$BF_4^-$. An identical workup gave **4f**$^+$$BF_4^-$ (0.250 g, 0.324 mmol, 88%) as a bright yellow powder. A sample was dissolved in CH_2Cl_2 and layered with ether. Small bronze prisms of **4f**$^+$$BF_4^-$ formed: mp 201–205 °C dec. Anal.[58]

[(η^5-C_5H_5)Re(NO)(PPh$_3$)(O=CH-4-C_6H_4F)]$^+$$BF_4^-$ (4g$^+$$BF_4^-$). Complex **5** (0.238 g, 0.427 mmol), CH_2Cl_2 (3 mL), HBF_4·OEt_2 (0.064 mL, 0.47 mmol), and *p*-fluorobenzaldehyde (0.137 mL, 1.28 mmol) were combined in a procedure analogous to that given for **4a**$^+$$BF_4^-$. An identical workup gave **4g**$^+$$BF_4^-$ (0.309 g, 0.410 mmol, 96%) as a bright yellow powder. A sample was dissolved in CH_2Cl_2 and layered with

(52) (a) Bullock, R. M.; Ricci, J. S.; Szalda, D. J. *J. Am. Chem. Soc.* **1989**, *111*, 2741. (b) For a tungsten–σ-acrolein complex (C=O 1.23(3) Å), see: Honeychuck, R. V.; Bonnensen, P. V.; Farahi, J.; Hersh, W. H. *J. Org. Chem.* **1987**, *52*, 5293.

(53) Anderson III, G. M.; Kollman, P. A.; Domelsmith, L. N.; Houk, K. N. *J. Am. Chem. Soc.* **1979**, *101*, 2344.

(54) Dalton, D. M.; Garner, C. M.; Fernández, J. M.; Gladysz, J. A. *J. Org. Chem.* **1991**, *56*, 6823.

(55) Klein, D. P.; Gladysz, J. A. *J. Am. Chem. Soc.* **1992**, *114*, 8710.

(56) Buhro, W. E.; Zwick, B. D.; Georgiou, S.; Hutchinson, J. P.; Gladysz, J. A. *J. Am. Chem. Soc.* **1988**, *110*, 2427.

(57) (a) Fetizon, M.; Henry, Y.; Moreau, N.; Moreau, G.; Golfier, M.; Prange, T. *Tetrahedron* **1973**, *29*, 1011. (b) Corey, E. J.; Suggs, J. W. *Tetrahedron Lett.* **1975**, *16*, 2647.

(58) Microanalytical data (C,H; Cl for solvates) are summarized in Table V1 (supplementary material).

ether. Small bronze prisms of **4g**$^+$BF$_4^-$ formed: mp 187–188 °C dec. Anal.[58]

[(η^5-C_5H_5)Re(NO)(PPh$_3$)(O=CHC$_{10}$H$_7$)]$^+$BF$_4^-$ (**4h**$^+$BF$_4^-$). Complex **5** (0.205 g, 0.368 mmol), CH_2Cl_2 (3 mL), HBF_4·OEt_2 (0.055 mL, 0.41 mmol), and 1-naphthaldehyde (0.150 mL, 1.10 mmol) were combined in a procedure analogous to that given for **4a**$^+$BF$_4^-$. The cooling bath was removed, and after 1 h, solvent was removed under oil pump vacuum. The resulting dark red foam was washed with ether and dissolved in CH_2Cl_2 (20 mL). The solution was added to ether (150 mL) with stirring. A flocculent salmon solid precipitated. With continued stirring, the precipitate slowly became a bright yellow powder. The powder was collected by filtration, washed with ether (3 × 10 mL), and dried under oil pump vacuum to give **4h**$^+$BF$_4^-$ (0.247 g, 0.314 mmol, 85%): mp 189–191 °C dec. Anal.[58]

[(η^5-C_5H_5)Re(NO)(PPh$_3$)(O=CHC$_6$H$_5$)]$^+$X$^-$ (**4i**$^+$X$^-$). **A.** Complex **5** (0.218 g, 0.391 mmol), CH_2Cl_2 (3 mL), HBF_4·OEt_2 (0.058 mL, 0.43 mmol), and benzaldehyde (0.119 mL, 1.17 mmol) were combined in a procedure analogous to that given for **4a**$^+$BF$_4^-$. An identical workup gave **4i**$^+$BF$_4^-$ (0.428 g, 0.581 mmol, 98%) as a bright yellow powder: mp 201–205 °C dec. Anal.[58] **B.** Complex **7** (0.219 g, 0.402 mmol), CH_2Cl_2 (5 mL), $Ph_3C^+PF_6^-$ (0.156 g, 0.402 mmol), and benzaldehyde (0.123 mL, 1.206 mmol) were combined in a procedure analogous to that given for **4b**$^+$PF$_6^-$. An identical workup gave **4i**$^+$PF$_6^-$ (0.281 g, 0.353 mmol, 88%) as a bright yellow powder: mp 210–214 °C dec. Anal.[58]

[(η^5-C_5H_5)Re(NO)(PPh$_3$)(O=CH-3,4,5-C_6H_2(OCH$_3$)$_3$)]$^+$BF$_4^-$ (**4j**$^+$BF$_4^-$). Complex **5** (0.319 g, 0.571 mmol), CH_2Cl_2 (5 mL), HBF_4·OEt_2 (0.085 mL, 0.63 mmol), and 3,4,5-trimethoxybenzaldehyde (0.351 g, 1.79 mmol) were combined in a procedure analogous to that given for **4a**$^+$BF$_4^-$. The cooling bath was removed, and after 1 h, the solution was added to ether (125 mL) with stirring. A flocculent salmon solid precipitated. Upon continued stirring, the precipitate became a bright yellow powder. The powder was collected by filtration, washed with ether (3 × 10 mL), and dried under oil pump vacuum to give **4j**$^+$BF$_4^-$ (0.426 g, 0.515 mmol, 90%): mp 168–169 °C dec. Anal.[58]

[(η^5-C_5H_5)Re(NO)(PPh$_3$)(O=CH-4-$C_6H_4C_6H_5$)]$^+$BF$_4^-$ (**4k**$^+$BF$_4^-$). Complex **5** (0.214 g, 0.383 mmol), CH_2Cl_2 (3 mL), HBF_4·OEt_2 (0.057 mL, 0.42 mmol), and *p*-phenylbenzaldehyde (0.210 mg, 1.15 mmol) were combined in a procedure analogous to that given for **4a**$^+$BF$_4^-$. The cooling bath was removed, and after 1 h, the solvent was removed under oil pump vacuum. The resulting dark red foam was washed with ether and dissolved in CH_2Cl_2 (20 mL). This solution was added to ether (150 mL) with stirring. A flocculent salmon solid precipitated, which was collected by filtration and triturated under ether. This gave a granular solid, which was washed with ether (3 × 10 mL) and dried under oil pump vacuum to give **4k**$^+$BF$_4^-$ (0.247 g, 0.314 mmol, 85%): mp 131–138 °C dec. Anal.[58]

[(η^5-C_5H_5)Re(NO)(PPh$_3$)(O=CH-4-$C_6H_4CH_3$)]$^+$BF$_4^-$ (**4l**$^+$BF$_4^-$). Complex **5** (0.229 g, 0.409 mmol), CH_2Cl_2 (3 mL), HBF_4·OEt_2 (0.061 mL, 0.45 mmol), and *p*-methylbenzaldehyde (0.145 mL, 1.23 mmol) were combined in a procedure analogous to that given for **4a**$^+$BF$_4^-$. An identical workup gave **4l**$^+$BF$_4^-$·$(CH_2Cl_2)_{0.5}$ (0.282 g, 0.356 mmol, 87%) as a bright yellow powder: mp 178–181 °C dec. Anal.[58] A sample was dissolved in CH_2Cl_2, layered with ether, and kept at −24 °C. Small bronze prisms of **4l**$^+$BF$_4^-$·$(CH_2Cl_2)_{0.5}$ formed: mp 168–176 °C dec. The presence of the solvate was verified by ^{1}H NMR (δ 5.30 (s) vs Si(CH$_3$)$_4$, $CDCl_3$). Anal.[58]

[(η^5-C_5H_5)Re(NO)(PPh$_3$)(O=CH-2,4-C_6H_3(OCH$_3$)$_2$)]$^+$BF$_4^-$ (**4m**$^+$BF$_4^-$). Complex **5** (0.205 g, 0.368 mmol), CH_2Cl_2 (3 mL), HBF_4·OEt_2 (0.055 mL, 0.40 mmol), and 2,4-dimethoxybenzaldehyde (0.188 mL, 1.13 mmol) were combined in a procedure analogous to that given for **4a**$^+$BF$_4^-$. An identical workup gave burgundy microcrystals of **4m**$^+$BF$_4^-$·$(CH_2Cl_2)_{0.5}$ (0.269 g, 0.321 mmol, 87%): mp 186–191 °C dec. Anal.[58] A sample was dissolved in CH_2Cl_2, layered with ether, and kept at −24 °C. This gave polymorphous burgundy plates of **4m**$^+$BF$_4^-$·$(CH_2Cl_2)_{0.5}$: mp 165–169 °C dec. Anal.[58] The presence of the solvate in both samples was verified by ^{1}H NMR (δ 5.30 (s) vs Si(CH$_3$)$_4$, $CDCl_3$).

[(η^5-C_5H_5)Re(NO)(PPh$_3$)(O=CH-3,4-C_6H_3(OCH$_3$)$_2$)]$^+$BF$_4^-$ (**4n**$^+$BF$_4^-$). Complex **5** (0.203 g, 0.363 mmol), CH_2Cl_2 (3 mL), HBF_4·OEt_2 (0.054 mL, 0.40 mmol), and 3,4-dimethoxybenzaldehyde (0.183 g, 1.09 mmol) were combined in a procedure analogous to that given for **4a**$^+$BF$_4^-$. An identical workup gave **4n**$^+$BF$_4^-$ (0.263 g, 0.330 mmol, 91%) as a burgundy powder: mp 199–201 °C dec. Anal.[58]

[(η^5-C_5H_5)Re(NO)(PPh$_3$)(O=CH-4-C_6H_4OCH$_3$)]$^+$X$^-$ (**4o**$^+$X$^-$). **A.** Complex **5** (0.223 g, 0.399 mmol), CH_2Cl_2 (3 mL), HBF_4·OEt_2 (0.060 mL, 0.44 mmol), and *p*-methoxybenzaldehyde (0.146 mL, 1.20 mmol) were combined in a procedure analogous to that given for **4a**$^+$BF$_4^-$. An identical workup gave **4o**$^+$BF$_4^-$·$(CH_2Cl_2)_{0.5}$ (0.278 g, 0.344 mmol, 86%) as a burgundy powder: mp 146–151 °C dec. Anal.[58] A sample was dissolved in CH_2Cl_2, layered with ether, and kept at −24 °C. This gave burgundy prisms of **4o**$^+$-BF$_4^-$·$(CH_2Cl_2)_{0.5}$: mp 145–149 °C dec. Anal.[58] **B.** Complex **7** (0.221 g, 0.406 mmol), CH_2Cl_2 (5 mL), Ph_3C^+ PF_6^- (0.158 g, 0.406 mmol), and *p*-methoxybenzaldehyde (0.148 mL, 1.22 mmol) were combined in a procedure analogous to that given for **4b**$^+$-PF$_6^-$. An identical workup gave **4o**$^+$PF$_6^-$·$(CH_2Cl_2)_{0.5}$ (0.302 g, 0.349 mmol, 86%) as a burgundy powder. A sample was dissolved in CH_2Cl_2, layered with ether, and kept at −24 °C (2 days). This gave **4o**$^+$PF$_6^-$·$(CH_2Cl_2)_{0.5}$ as burgundy prisms: mp 136–142 °C dec. Anal.[58]

IR Equilibrium Measurements. IR spectra of **4**$^+$BF$_4^-$ were recorded in CH_2Cl_2 (absorbance mode, 0.01–0.04 M). Data for **4i,l,o**$^+$BF$_4^-$ were obtained in a thermostated cell.[29] The remaining data were acquired in standard solution cells at 26 °C (thermocouple reading from spectrometer cavity). Absorptions were assumed to be Gaussian about λ_{max}. Thus, for overlapping peaks, the area of the unoccluded half was taken as proportional to concentration. Masses of peak halves were determined in triplicate.

Crystal Structure of 4o$^+$**PF**$_6^-$·$(CH_2Cl_2)_{0.5}$. A burgundy prism was mounted for data collection on a Syntex P$\bar{1}$ diffractometer as summarized in Table V. Cell constants were obtained from 29 reflections with 10° ≤ 2θ ≤ 30°. Lorentz, polarization, empirical absorption (Ψ scans), and decay (12.04%) corrections were applied to the data. The structure was solved by standard heavy-atom techniques with the SDP/VAX package.[59] Non-hydrogen atoms were refined with anisotropic thermal parameters, and hydrogen atom positions were calculated. Scattering factors, and $\Delta f'$ and $\Delta f''$ values, were taken from the literature.[60]

Acknowledgment. We thank the DOE for support of this research and Dr. W. Woolfenden for the CPMAS ^{13}C NMR spectra.

Supplementary Material Available: Tables of microanalytical data for **4a-o**$^+$X$^-$,[58] bond lengths and angles, atomic coordinates, and anisotropic thermal parameters for **4o**$^+$PF$_6^-$·$(CH_2Cl_2)_{0.5}$ (4 pages); calculated and observed structure factors for **4o**$^+$PF$_6^-$·$(CH_2Cl_2)_{0.5}$ (14 pages). Ordering information is given on any current masthead page.

(59) Frenz, B. A. The Enraf-Nonius CAD 4 SDP—A Real-time System for Concurrent X-ray Data Collection and Crystal Structure Determination. In *Computing and Crystallography*; Schenk, H., Olthof-Hazelkamp, R., van Konigsveld, H., Bassi, G. C., Eds.; Delft University Press: Delft, Holland, 1978; pp 64–71.

(60) Cromer, D. T.; Waber, J. T. In *International Tables for X-ray Crystallography*; Ibers, J. A., Hamilton, W. C., Eds.; Kynoch: Birmingham, England, 1974; Volume IV, pp 72–98, 149–150; Tables 2.2B and 2.3.1.